# Distinctive and complementary roles of E2F transcription factors during plant replication stress responses

Maherun Nisa, Thomas Eekhout, Clara Bergis, Jose-Antonio Pedroza-Garcia, Xiaoning He, Christelle Mazubert, Ilse Vercauteren, Toon Cools, Rim Brik-Chaouche, Jeannine Drouin-Wahbi, et al.

# Distinctive and complementary roles of E2F transcription factors during plant replication stress responses

Maherun Nisa,[1,2,‡] Thomas Eekhout,[3,4] Clara Bergis,[1,2] Jose-Antonio Pedroza-Garcia,[3,4] Xiaoning He,[1,2] Christelle Mazubert,[1,2] Ilse Vercauteren,[3,4] Toon Cools,[3,4] Rim Brik-Chaouche,[1,2] Jeannine Drouin-Wahbi,[1,2], Layla Chmaiss[1,2], David Latrasse,[1,2] Catherine Bergounioux,[1,2] Klaas Vandepoele,[3,4] Moussa Benhamed,[1,2] Lieven De Veylder[3,4, †] and Cécile Raynaud[1,2,*, †]

[1] Université Paris-Saclay, CNRS, INRAE, Université Evry, Institute of Plant Sciences Paris-Saclay (IPS2), 91190, Gif sur Yvette, France

[2] Université de Paris Cité, CNRS, INRAE, Institute of Plant Sciences Paris-Saclay (IPS2), 91190, Gif sur Yvette, France

[3] Department of Plant Biotechnology and Bioinformatics, Ghent University, Ghent, B-9052, Belgium.

[4] Center for Plant Systems Biology, VIB, Ghent, B-9052, Belgium

[‡] Present address: Plant Molecular and Cellular Biology Laboratory, Salk Institute for Biological Studies, La Jolla, 92037, USA.

[†] Senior author

*Author for correspondence: cecile.raynaud@universite-paris-saclay.fr

**SHORT TITLE:** E2FA and E2FB differently participate in the DDR

**SHORT SUMMARY:** Here, we investigated the respective roles of E2FA and E2FB transcription factors during the response to replication stress. We show that they function together with SOG1 to control the expression of DDR genes, and that E2FB plays a unique role in allowing cell cycle progression from G2/M in spite of replication stress.

**CONTACT:** cecile.raynaud@universite-paris-saclay.fr

## Abstract

Survival of living organisms is fully dependent on their maintenance of genome integrity, being permanently threatened by replication stress in proliferating cells. Although the plant DNA damage response (DDR) regulator SOG1 has been demonstrated to cope with replicative defects, accumulating evidence points to other pathways functioning independently of SOG1. Here, we have studied the role of the Arabidopsis E2FA and EF2B transcription factors, two well-characterized regulators of DNA replication, in the response to replication stress. Through a combination of reverse genetics and chromatin-immunoprecipitation approaches, we show that E2FA and E2FB share many target genes with SOG1, providing evidence for their involvement in the DDR. Analysis of double and triple mutant combinations revealed that E2FB, rather than E2FA, plays the most prominent role in sustaining growth in the presence of replicative defects, either operating antagonistically or synergistically with SOG1. Reversely, SOG1 aids in overcoming the replication defects of E2FA/E2FB-deficient plants. Our data reveal a complex transcriptional network controlling the replication stress response, in which both E2Fs and SOG1 act as key regulatory factors.

**Key Words**: Replication Stress, E2F, SOG1, Cell Cycle, Arabidopsis

## Introduction

In all eukaryotic organisms, faithful transmission of genetic information from one generation to the next strongly depends on accurate DNA replication. Several factors, including pyrimidine dimers, unrepaired DNA lesions, RNA–DNA hybrids and the formation of DNA secondary structures, can disrupt or slow down DNA replication. These factors can result in fork stalling, leading to replication stress that may in turn affect genomic integrity (Mazouzi et al., 2014). Due to the multiplicity of factors that can lead to fork stalling, replication stress is a ubiquitous threat to the maintenance of genome integrity in all proliferating cells. Interestingly, in plants, there is accumulating evidence that exposure to abiotic or biotic stresses can trigger the DNA damage response (DDR) (Nisa et al., 2019; Pedroza-Garcia et al., 2022), and this effect could partly be due to an increased replication stress (Nisa et al., 2021).

In eukaryotes, the DDR signaling cascade is largely conserved and activates checkpoints that induce a cell cycle arrest until the damaged DNA is repaired. The DDR is activated by DNA double-strand breaks (DSBs) or replication stress, and relies on the two protein kinases ATAXIA TELANGIECTASIA MUTATED (ATM) and ATM AND RAD3- RELATED (ATR), respectively (Maréchal and Zou, 2013). In animal and yeast cells, when the progression of DNA replicative polymerases is hindered, REPLICATION PROTEIN A (RPA)-coated single-stranded DNA accumulates, resulting in the recruitment and activation of ATR (Saldivar et al., 2017) through mechanisms that appear to be conserved in plants (Sweeney et al., 2009). By contrast, downstream signaling events differ between plants and animals. In plants, ATR is thought to directly phosphorylate the central DDR transcriptional regulator SUPPRESSOR OF GAMMA-RESPONSE 1 (SOG1), which in turns activates DNA repair genes and negative regulators of cell cycle progression, such as WEE1 (Preuss and Britt, 2003; De Schutter et al., 2007; Sjogren et al., 2015; Bourbousse et al., 2018). However, when treated with hydroxyurea (HU), which triggers replication stress by depleting the intracellular dNTP pool, *wee1 sog1* double mutants display a stronger growth inhibition than the corresponding single mutants, indicating that SOG1 and WEE1 function partially independently to control the replication stress response (Hu et al., 2015). Likewise, hypomorphic mutants of the replicative DNA polymerase ε (Polε) catalytic subunit POL2A show a constitutive activation of the replication stress response that is only partially dependent on SOG1. Indeed, ATR and WEE1 are crucial for the survival of *pol2a*, but the *pol2a sog1* double mutant is viable, and still shows activation

of a subset of DDR genes (Pedroza-Garcia et al., 2017), indicating that part of the transcriptional response evoked by replication stress is controlled by a yet unidentified transcription factor.

Seen their role as transcriptional activators of genes required for S-phase progression, possible contributors to the transcriptional reprograming induced by replication stress could be E2F transcription factors. Among other functions, the E2Fs–RBR1 (RETINOBLASTOMA RELATED 1) module plays a well-known role in the control of DNA replication (Müller et al., 2001; Vlieghe et al., 2003; Vandepoele et al., 2005; Naouar et al., 2009). When a plant cell receives mitogenic cues, D-type cyclin-activated cyclin-dependent kinases phosphorylate RBR1, which unleashes E2F activity. In *Arabidopsis,* the E2F family comprises six members which are E2FA, E2FB, E2FC, DEL1/E2Fe, DEL2/E2Fd, and DEL3/E2Ff (Vandepoele et al., 2002). They are categorized into canonical E2Fs (E2FA, E2FB and E2FC) that function as heterodimers with their dimerization partners DPA and DPB, and non-canonical E2Fs (DEL1/E2Fe, DEL2/E2Fd and DEL3/E2Ff) that operate independently of dimerization partners (Mariconti et al., 2002; Lammens et al., 2009). Canonical E2FA and E2FB are considered as transcriptional activators because they contain a transactivation domain and stimulate S-phase entry, whereas E2FC is generally considered as a repressor (De Veylder et al., 2002; del Pozo et al., 2002; Mariconti et al., 2002; Sozzani et al., 2006; Lammens et al., 2009). E2FA and E2FB are thought to be partially redundant, because single mutants of *E2FA* and *E2FB* show no dramatic phenotypes (Yao et al., 2018; Őszi et al., 2020), whereas a double mutant is lethal (Li et al., 2017). However, some differences exist between E2FA and E2FB. For example, E2FA and E2FB play different roles in the growth inhibition triggered by UV-B exposure (Gómez et al., 2022). In addition, E2FB, together with E2FC and RBR1, was found to be a part of DREAM (DP, Rb-like, E2F, and MuvB) complexes, which are crucial for the timely succession of transcriptional waves involved in cell cycle progression and/or onset of cell differentiation (Magyar et al., 2016; Lang et al., 2021). By contrast, E2FA is not copurified with DREAM complex subunits from plant cell extracts, although it can interact with some components in the yeast two-hybrid system, suggesting that it differs from E2FB in the strength of its association to DREAM complexes (Lang et al., 2021).

In addition to their role as cell cycle regulators, several lines of evidence indicate that E2Fs control the cellular response to DNA damage and replication stress. In mammals, *E2F1* transcription is usually inactivated at the start of the S-phase by the induction of the repressive E2F6 protein, which is an E2F1 target (Giangrande et al., 2004). However, under DNA damaging conditions, the E2F1 protein is stabilized by ATM- or ATR-dependent

phosphorylation (Lin et al., 2001) and accumulates at the sites of DSBs (Biswas and Johnson, 2012). Additionally, during replication stress, the E2F6 repressor is inactivated, causing sustained *E2F1* transcription that is necessary for the arrest and stabilization of replication forks and in this way prevents DNA damage (Bertoli et al., 2013; Bertoli et al., 2016). Remarkably, in cells with an impaired checkpoint control, the sustained transcription of *E2F1* is sufficient to alleviate DNA damage levels (Bertoli et al., 2016). Likewise, in tobacco BY-2 cells, the *NtE2F* gene is induced in response to high doses of UV-C (Lincker et al., 2004) and its protein localizes in distinct chromatin foci upon DNA damage (Lang et al., 2012), hinting at a possible conservation of the role of E2F transcription factors in the DDR in plants. More recently, it was found that upon DNA damage, RBR1 also colocalizes with γH2AX, a histone variant that is phosphorylated by ATM and ATR and forms foci delineating breaks in the DNA (Friesner et al., 2005), and that this is necessary for correct localization of RAD51 foci (Biedermann et al., 2017). Using chemical inhibitors of ATM and ATR, it was also found that the formation of foci of E2FA and RBR1 is dependent on both kinases (Horvath et al., 2017), recruiting the DNA repair protein BRCA1 to these foci. Furthermore, E2FB was shown to be required for cell cycle arrest induced by the crosslinking agent cisplatin (Lang et al., 2021). Collectively, these results provide strong evidence for the role of E2FA and E2FB in the cellular response to DSBs, although their contribution to the replication stress response has never been explored.

In this study, we studied the involvement of E2FA and E2FB in response to replication stress. Surprisingly, we show that E2FA and E2FB share numerous targets with SOG1. Further, we show that E2FB, rather than E2FA, activity is required to allow cell cycle progression despite replication stress. In-depth analysis of the expression behavior of common SOG1 and E2F targets demonstrates that E2FA and E2FB play both complementary and distinct roles in this pathway.

## Results

### E2FA and E2FB share targets with SOG1

E2FA, E2FB and RBR1 have all recently been shown to play a role in the plant's DSB response (Biedermann et al., 2017; Horvath et al., 2017; Lang et al., 2021). Exploiting our recent analysis of E2FA and E2FB targets (Gombos et al., 2022), we investigated whether E2FA/B shared common targets with SOG1. When comparing the target genes of E2FA (Supplemental Table S1A), E2FB (Supplemental Table S1B) and SOG1 as determined by tandem chromatin affinity

purification (TChAP) (Verkest et al., 2014) or chromatin immunoprecipitation followed by sequencing (ChIP-seq) experiments (Bourbousse et al., 2018; Gombos et al., 2022), we found that a greater number of SOG1 target genes was also targeted by at least one of the two E2F transcription factors than what would be expected by chance (Fisher's exact test, Figure 1A, Supplemental Table S1C). Among these, the *WEE1* gene could be found, encoding a cell cycle inhibitory kinase implicated in the replication stress response (De Schutter et al., 2007). Interestingly, residual activation of the *WEE1* promoter was observed in response to HU-induced replication stress in a *sog1* mutant and required the E2F-binding site found in its promoter, confirming a potential involvement of E2FA/B in the replication stress response (Figure 1F). We next compared the position of experimentally identified E2FA- and E2FB-binding sites with those previously identified for SOG1 (Bourbousse et al., 2018). Both E2FA and E2FB bound the common target genes at positions close to the SOG1-binding site (Figure 1B-E, Supplemental Table S1C), suggesting that E2FA/B and SOG1 bind in close proximity to each other on their target promoters. The observation that E2FA/B can activate *WEE1* in response to HU independently of SOG1 (Figure 1F) and the significant overlap between putative E2FA/B and SOG1 target genes (Figure 1A) prompted us to test whether E2FA/B play a role in the replication stress response.

**Loss of E2FB strongly aggravates growth defects triggered by replication stress**

To explore the role of E2FA and E2FB in the replication stress response, we used the hypomorphic mutant for DNA polymerase ε (Polε), *pol2a-4* (hereafter referred to as *pol2a*) that shows constitutive replication stress (Pedroza-Garcia et al., 2017), and generated double and triple mutant combinations between *pol2a*, *sog1* and *e2fa* or *e2fb* mutants. Two independent T-DNA insertion lines have been described for both *E2FA* and *E2FB* (Berckmans et al., 2011a; Berckmans et al., 2011b). In the case of *E2FA*, the *e2fa-1* allele appears to be a null mutant lacking E2FA protein accumulation, whereas *e2fa-2* accumulates significant levels of a truncated protein (Leviczky et al., 2019). In the case of *E2FB*, the protein cannot be detected in protein extracts of either *e2fb-1* or *e2fb-2* mutants (Leviczky et al., 2019). In terms of protein function, viable *e2fa e2fb* double mutants have been obtained using the *e2fa-2* but not the *e2fa-1* allele (Heyman et al., 2011), suggesting that the truncated protein accumulating in *e2fa-2* mutants is at least partially functional. For our genetic analysis, we therefore used only the *e2fa-1* mutant allele, in which *E2FA* loss of function is likely full, and both *e2fb* alleles. Throughout

the manuscript, we show results obtained for the *e2fb-1* allele, but the *e2fb-2* allele systematically gave the same results. Phenotypically, *e2fa-1* and *e2fb-1* single mutants did not show a growth reduction compared with the wild type (Col-0), whereas *pol2a* mutants were significantly smaller (Figure 2A, B). Growth reduction was more severe in the *pol2a sog1* double mutant, consistent with the hypersensitivity of the *sog1* mutant to replication stress (Pedroza-Garcia et al., 2017). The *pol2a e2fa-1* mutant rosette size was identical to that of the *pol2a* parent, whereas the *e2fb-1 pol2a* mutant was slightly smaller. Strikingly, the *e2fb-1 pol2a sog1* triple mutant showed a more severe growth defect than *pol2a sog1*, a phenomenon not observed with the *e2fa-1* mutation (Figure 2A, B). We also analyzed the root length of the various mutants, and observed that E2FB, but not E2FA, is required for root growth in plants suffering from constitutive replication stress (Figure 2C). These data show that E2FB contributes to the plant's response to replication stress, allowing growth maintenance despite the replication defects.

## E2FB positively regulates meristem size and cell cycle progression in response to replication stress

The severe growth reduction observed in *e2fb-1 pol2a sog1* triple mutants, and to a lesser extent, in *e2fb-1 pol2a* double mutants, likely results from cell proliferation defects. To test this hypothesis, we first measured the root meristem size in all genotypes. As shown in Figure 3, replication stress triggered by Polε deficiency resulted in a reduced meristem size. Whereas this defect was not significantly aggravated in the absence of SOG1, root meristem length was further reduced in *ef2b-1 pol2a* and *e2fb-1 pol2a sog1* mutants (Figure 3B). Again, this effect was not observed in *e2fa-1 pol2a* and *e2fa-1 pol2a sog1* mutants (Figure 3B). These results confirmed that E2FB, but not E2FA, plays a crucial role in proliferating cells to protect them from cell proliferation arrest triggered by replication stress.

To further dissect how E2FB affects cell proliferation in response to replication stress, we decided to analyze cell cycle progression into more detail in all mutant combinations. We first analyzed cell cycle progression in root meristems using cumulative EdU incorporation (Hayashi et al., 2013), but EdU positive cells represented a very large proportion of cells in the meristem of *e2fb-1 pol2a sog1* triple mutant, and this proportion increased very slowly, making S-phase and cell cycle length calculation extremely difficult (Supplemental Figure S1). As a proxy for S-phase length, we therefore assessed the proportion of S-phase cells using short EdU labelling

(30 min). Delayed S-phase progression causes S-phase to account for a larger proportion of total cell cycle length and thus results in an increase in the proportion of S-phase cells in the cell population. The proportion of nuclei in S-phase was the same in the wild type, single *sog1*,*e2fa-1* and *e2fb-1* mutants, and in the double *e2fa-1 sog1* and *e2fb-1 sog1* mutants (Figure 3C) while it increased in all mutant combinations holding the *pol2a* mutation, consistent with our previous findings (Pedroza-Garcia et al., 2017). Interestingly, it further increased in *pol2a sog1* and *e2fb1 pol2a* mutants, and even more so in the *e2fb-1 pol2a sog1* triple mutant. By contrast, the *e2fa1* mutation had no impact on the proportion of S-phase cells in any mutant combination. Next, to monitor G2 to M progression, we performed a pulse EdU labelling (30 min), followed by a 5 h thymidine chase (Figure 3D). Progression from G2 to M was delayed in *e2fb-1 pol2a* and even more so in *e2fb-1 pol2a sog1* mutants, compared to *pol2a* and *pol2a sog1* mutants respectively (Figure 3D). This phenomenon was not observed in *e2fa-1* mutant combinations. The same result was obtained using flow-cytometry on flower buds, as indicated by a significant increase in the population of G2 nuclei at the expense of number of G1 cells in the *e2fb-1 pol2a* and *e2fb-1 pol2a sog1* mutants, compared to the wild-type, that was not observed in *pol2a* and *pol2a sog1* (Supplemental Figure S2). These data indicate that the same cell cycle defects are observed in different types of proliferating tissues.

Together, these data suggest that E2FB positively regulates cell cycle progression through G2 and the onset of the G2/M transition in replicative-stress exposed cells. This function seems to be particularly important in the absence of SOG1, suggesting that SOG1 and E2FB may act in parallel to maintain the proliferative capacity in replication stress-exposed cells.

**Replicative stress-induced genes are under the dual control of E2Fs and SOG1**

To gain insight into the mechanisms underlying the role of E2FB in the replication stress response, we compared gene expression changes in shoot apices of *pol2a*, *pol2a sog1* and *e2fb-1 pol2a sog1* mutants (Supplemental Table S2). Compared with wild type plants, we found 1,822, 2,599 and 3,512 upregulated genes in *pol2a*, *pol2a sog1* and *e2fb-1 pol2a sog1* mutants, respectively (FDR < 0.05). Among those, 1,095 were commonly upregulated in all three mutant lines (Figure 4A, Supplemental Table S3). Gene Ontology (GO) analysis of these 1,095 genes revealed a significant enrichment in GO terms such as DNA repair, DNA replication, and negative regulation of the cell cycle (Figure 4B), consistent with the constitutive replication stress triggered by *POL2A* deficiency and induced cell cycle defects (Pedroza-Garcia et al.,

2017). Genes specifically upregulated in the *e2fb-1 pol2a sog1* mutant were not enriched in E2F target genes, indicating that most of them are likely indirectly regulated by E2Fs. Because DDR and cell cycle-related genes were enriched only in up-regulated genes, we focused on these genes for further analyses.

To understand the behavior of SOG1 target genes in the different genotypes, we analyzed into more detail their expression level in *pol2a*, *pol2a sog1* and *e2fb-1 pol2a sog1* mutants. Out of the 309 SOG1 targets (Bourbousse et al., 2018), 78 were significantly upregulated (FDR < 0.05, $\log_2$FC > 0.5) in at least one genotype compared with the wild type and were kept in the analysis. For each gene, we calculated a z-score based on its expression level in the different samples. This approach allowed us to define 3 main groups of genes with contrasted expression profiles (Figure 4C, Supplemental Table S4). The first group (comprising 19 genes) corresponded to genes mainly regulated by SOG1: they were induced in *pol2a*, but their expression returned to basal levels in *pol2a sog1* and *e2fb-1 pol2a sog1* mutants. Genes in group 2 were highly induced in *pol2a* mutants, had a lower expression in *pol2a sog1* mutants, but their expression was increased in the triple mutant compared to *pol2a sog1*, indicating that they are antagonistically regulated by SOG1 and E2FB (30 genes, Figure 4C, Table S4). Interestingly, group 2 genes were particularly enriched in E2F targets (about 60% of genes were identified as targets of at least one E2F, Supplemental Table S4), further supporting the hypothesis that they are under dual control of SOG1 and E2FB. Importantly, we could confirm by RT-qPCR on a sub-set of these genes that their expression was not affected by the *e2fa-1* mutation, supporting the hypothesis that they are specifically repressed by E2FB (Supplemental Figure S3). Among these shared E2FB/SOG targets that appeared to be antagonistically controlled by SOG1 and E2FB, we found the *ANAC044* and *ANAC085* transcription factor genes that have been shown to negatively regulate G2/M progression. This result was confirmed by RT-qPCR (Supplemental Figure S4A). Interestingly, *ANAC044* and *ANAC085* are not only direct SOG1 and E2FB targets, but also RBR1 targets ((Gombos et al., 2022), Supplemental Figure S4B, C), suggesting that E2FB could repress them through its interaction with RBR1. Since these two transcription factors have been involved in the inhibition of the G2/M transition, their up-regulation in *e2fb-1 pol2a sog1* mutants could account for the observed delay in G2 progression we observed in these mutants.

Finally, the transcriptomics results indicate that E2FA and E2FB could function redundantly to activate DDR genes independently of SOG1. Indeed, genes in group 3 (18 genes) were partially dependent on SOG1 for their induction, but their expression level remained high in triple

mutants (Figure 4C), indicating that they are activated independently of SOG1 and E2FB. In addition, the majority (about 60%) of group 3 genes were identified as E2F targets, suggesting that E2FA could account for their activation in the absence of SOG1 and E2FB. Reciprocally, SOG1 targets were significantly enriched amongst genes upregulated in the *e2fb-1 pol2a sog1* triple mutant compared with the *pol2a sog1* mutant (p =1.118e-5, Fisher's exact test, total number of genes detected in the RNA-Seq analysis = 20,946, Figure 4D), further confirming that *bona fide* SOG1 targets can be activated independently of SOG1 in response to replication stress. Interestingly, GO analysis of all genes that were specifically upregulated in *pol2a sog1* and *e2fb-1pol2a sog1* mutants and not in *pol2a* single mutants compared with wild-type plants revealed a significant enrichment in terms of related to cell cycle regulation (Supplemental Figure S5A), and E2FA and E2FB targets were significantly enriched in this list (Supplemental Figure S5B). It is worth noting that E2F targets were also highly enriched among genes that were commonly upregulated in all three mutant lines (428 out of 1,095, p = 8.179e-36, Fisher's exact test, total number of genes detected in the RNA-Seq analysis = 20,946). These observations suggest that although the *e2fa-1* mutation alone or in combination with *sog1* does not appear to affect the developmental defects caused by replication stress, E2FA could activate DDR genes, but likely functions redundantly with E2FB to fulfill this role.

Together, these results indicate intricate regulation of DDR genes by SOG1 and E2Fs in response to replication stress. On the one hand, E2FB plays an important role in mitigating DDR gene activation to allow sustained growth in response to replication stress and on the other hand, E2FA and E2FB likely function redundantly to activate a subset of DDR genes both synergistically and in parallel of SOG1.

## E2FA, E2FB and SOG1 cooperate to allow cell cycle progression in response to replication stress

To test the possibility that E2FA could contribute to the replication stress response in the absence of E2FB and SOG1, we used the partial loss-of-function allele of E2FA (*e2fa-2*), and generated *e2fa-2 e2fb-1 sog1* triple mutants. To induce replication stress, plantlets were exposed to the replication inhibitor HU. As published before, *sog1* mutants are slightly sensitive to replication stress (Hu et al., 2015), whereas *e2fa*, *e2fb* and *e2fa-2 e2fb-1* showed no such hypersensitivity (Figure 5). Both *e2fa* and *e2fb* mutant alleles behaved in the same way. Similarly, as observed in response to constitutive replication stress induced by the *pol2a* mutant

(Figure 2B), *e2fb-1 sog1* but not *e2fa-1 sog1* double mutants were more sensitive to HU than *sog1* mutants, consistent with the hypothesis that E2FB plays a more prominent role than E2FA in the replication stress response. Strikingly, the *e2fa-2 e2fb-1 sog1* triple mutant displayed even stronger HU hypersensitivity, with root growth being almost completely blocked after transfer on HU (Figure 5, Supplemental Figure S6), and cell death being induced in the root meristem as indicated by cellular uptake of propidium iodide (Supplemental Figure S7). It is worth noting that using HU induces milder developmental defects than the *pol2a* mutation, possibly because it affects mainly roots that are directly in contact with the medium, and because plants are kept on the drug for a short period of time. Nevertheless, these data clearly indicate a contribution of E2FA to the replication stress response when both E2FB and SOG1 are inactivated.

Because hindrance of fork progression is inevitable during the S-phase, we investigated whether E2F deficiency may trigger replication stress even in a wild-type background. Whereas Gómez et al. (2022) reported an increase in meristem size and cortical meristem cell number for the *e2fa-2 e2fb-1* mutant, under our own growth conditions we noticed no effect on meristem size but a statistical significant reduction in cell number (Supplemental Figure S8A-C), indicative for the activation of a cell cycle arrest. Although the inhibition of cell proliferation could be due to the role of E2Fs as activators of cell cycle progression, it may also reflect an inefficient response to basal levels of replication stress that generally happen during the S-phase. In line with this hypothesis, we found that *e2fa-2 e2fb-1* double mutants displayed a prolonged S-phase and increased total cell cycle length (Figure 6), whereas S and G2 phase duration was unaffected in *e2fa-2* or *e2fb-1* single mutants (Supplemental Figure S8 D-E). Importantly, these defects were abolished in the *sog1* mutant background, indicating that E2F deficiency triggers replication stress leading to a SOG1-dependent cell cycle delay. To confirm this hypothesis, we performed an RNA-Seq analysis on root tips of 7-day-old seedlings grown under control conditions. A total of 148 genes were found to be downregulated in the *e2fa-2 e2fb-1* mutant (FDR < 0.01), of which 73 are likely direct E2FA or E2FB target genes based on ChIP data (Figure 6C, Supplemental Table S5A, B). This list includes described components of the DNA replication machinery (Supplemental Table S6), and GO enriched categories (obtained through http://geneontology.org/), including DNA replication initiation, DNA duplex unwinding and chromatin assembly (Supplemental Table S7). Next to the 148 downregulated genes, we found 345 genes to be upregulated (FDR < 0.01, FC > 1.5). Strikingly, according to ChIP data 145 of these are E2FA- or E2FB-bound genes (Figure 6C, Supplemental Table S5C), consistent with

recent evidence that the canonical E2FA/B play a key role in the repression of cell cycle genes, likely through their association with RBR1 (Gombos et al., 2022). GO categories enriched in the list of E2F-bound upregulated genes mainly indicate DNA repair, recombinational repair and response to gamma irradiation and X-ray (Supplemental Table S8). Quantitative RT-PCR of a selected number of genes from both down- and upregulated genes confirmed the results from the RNA-Seq (Figure 6D, E). Strikingly, upregulated *PARP1* and *SMR7* gene expression in the *e2fa-2 e2fb-1* double mutant was repressed in the *e2fa-2 e2fb-1 sog1* triple mutant. Differently to the *MCM9* gene that showed no transcriptional repression, the former two are *bona fide* SOG1 target genes, indicative that absence of E2FA and E2FB triggers a SOG1 dependent transcriptional response (Figure 6E). Accordingly, among the 345 genes upregulated in *e2fa-2 e2fb-1* double mutants, 43 were SOG1 targets (a number significantly greater than could be expected by chance, p = 7.746e-24, Fisher's exact test, total number of genes detected in the RNA-Seq experiment = 17,028), further confirming that loss of E2FA and E2FB triggers replication stress and SOG1-dependent activation of DDR genes.

## DISCUSSION

E2Fs are core cell cycle regulators that are evolutionarily conserved over most multicellular eukaryotes, including animals and the green lineage (Bertoli et al., 2013). Although functional diversification of E2Fs has been described into details in animals (Ishida et al., 2001), our understanding of plant E2Fs' specific functions remains limited.

### E2FB plays a more prominent role than E2FA to allow plant growth in response to replication stress

Based on our observation that the Arabidopsis E2FA and E2FB transcription factors share several target genes with the central DDR regulator SOG1, we investigated their contribution to the plant's replication stress response. We found that loss of E2FB, but not of E2FA, severely aggravated the developmental defects of the *pol2a-4* mutant that suffers from constitutive replication stress (Pedroza-Garcia et al., 2017), as well as the sensitivity of the *sog1* mutant to the DNA-replication blocking drug HU. This requirement for E2FB for replication stress tolerance was particularly obvious in the *sog1* background, suggesting that E2FB and SOG1 act in parallel to cope with replication defects (Figure 7A). At the cellular level, we observed

that progression from S to M was slower in these lines, suggesting that the length of the G2 phase was increased by E2FB loss of function. Together, our results suggest that E2FB could allow the progression of cells through G2/M under replication stress conditions.

We found that negative regulators of the cell cycle such as *ANAC044* and *ANAC085* are upregulated in *e2fb-1 pol2a sog1* mutants compared with *pol2a sog1* mutants, suggesting that E2FB may allow G2 to M progression by inhibiting the repressors of the G2/M transition. Importantly, a role in allowing sustained cell proliferation in response to replication stress seems specific to E2FB, since loss of E2FA did neither alter the sensitivity of *sog1* mutants to HU, nor affect plant growth, meristem size or the proportion of G2 cells in the *pol2a* or *pol2a sog1* mutants. These non-overlapping roles could relate to the fact that E2FB is more tightly associated to DREAM complexes than E2FA (Magyar et al., 2016; Lang et al., 2021). The function of these complexes is to bring together transcription factors that control G1/S genes (E2Fs) with the transcription factors controlling G2/M genes (MYB3Rs), which is essential for the timely succession of transcriptional waves during the cell cycle and entry into quiescence during differentiation (Magyar et al., 2016). DREAM complexes could thus be required to maintain the proliferative capacity of cells during replication stress by repressing the expression of cell cycle inhibitory factors such as *ANAC044* and *ANAC085* (Figure S4) or *SMR5* (Table S4).

Nevertheless, *e2fa-2 e2fb-1 sog1* triple mutants were completely unable to grow in the presence of replication stress, indicating that E2FA also contributes to this cellular response. We propose that E2FA and E2FB could function redundantly to activate part of the DDR response. This hypothesis would explain the fact that a large set of DDR and cell-cycle related genes remain highly expressed in *e2fb-1 pol2a sog1* triple mutants. Importantly, the *e2fa-2* allele has been described as missing the transactivation and RBR1-interaction domain but retaining the "marked box" domain, which in mammals can provide a secondary interaction interface with RBR1 (Horvath et al., 2017), and still represses expression of DDR genes such as *BRCA1*, in contrast to the *e2fa-1* allele that misses this interaction domain. We therefore cannot rule out the possibility that the dramatic phenotype of the *e2fa-2 e2fb-1 sog1* mutant could be due to the inhibition of E2F target genes through binding of the residual E2FA in a complex with RBR1.

**Complex transcriptional networks underlie the role of E2FA/B and SOG1 in the replication stress response**

A remarkable finding in this study is that activating E2FA/B and SOG1 induces a large set of common targets. Dual control of DDR genes by activating E2FA/B and SOG1 may allow fine-tuning of the gene expression level according to the replication stress intensity. E2FA/B activity might account for basal induction levels during the S-phase, when cells are expected to be most sensitive to replication inhibitory stresses, whereas SOG1 might account for further activation in response to fork stalling. Likewise, in the *e2fa-2 e2fb-1* double mutant, we did not only see many E2F target genes being transcriptionally repressed, but an even higher number of target genes to be induced, consistent with the notion that E2FA and E2FB largely function as corepressors by recruiting RBR1 to their targets (Gombos et al., 2022). 43 of these genes are SOG1 target genes, including *BRCA1* and *RAD51*. We hypothesize that these E2F target genes are essential for S-phase progression as well as for repair of stalled replication forks, and that in the *e2fa-2 e2fb-1* plants, SOG1 is activated because of replication defects. Such dual control of target genes by both E2FA/B and SOG1 might explain the additive effects of the *e2fb-1* and *sog1* mutations seen on growth and cell cycle progression in the *pol2a* mutant, as well as the increased sensitivity of the *e2fb-1 sog1* and *e2fb-2 sog1* double and *e2fa-2 e2fb-1 sog1* triple mutants towards HU. It probably also accounts for the almost complete stalling of cell cycle progression of the *e2fa-2 e2fb-1 sog1* triple mutant in the presence of HU. Another hypothesis that could explain the hypersensitivity of the *e2fa-2 e2fb-1 sog1* triple mutant to HU is the role of E2FA in DSB repair (Biedermann et al., 2017; Horvath et al., 2017). Defects in the replication stress response triggered by SOG1 and E2FB deficiency could lead to a failure of fork stabilization mechanisms and accumulation of DSBs, which would require E2FA activation for repair.

Thus, the transcriptional network activated under replication stress is likely to be quite complex. Indeed, although E2FB and SOG1 share target genes, they seem to have opposite effects on the expression of a significant proportion of their common targets. According to our transcriptomic analysis, we can distinguish three classes of genes amongst the SOG1-regulated DDR genes (Figure 7B). A first set of genes seems to depend almost exclusively on SOG1 for their expression, as their induction is lost in *pol2a sog1* end *e2fb-1 pol2a sog1* plants (Figure 7B, class A genes). Consistently, this group of genes (corresponding to cluster 1 on Figure 4), is not statistically enriched in E2FA/B targets. By contrast, class B genes appear to be antagonistically regulated by SOG1 and E2FB, since their expression is lower in *pol2a sog1* mutants than in *e2fb-1 pol2a sog1* mutants. This is the case for example for *ANAC044* and *ANAC085* (Figure 7B, inset). Together with the fact that these two genes are also identified as direct RBR1 targets,

this observation suggests that the repressor role of the E2FB–RBR1 complex, which we have recently described to be essential for the maintenance of cell cycle quiescence (Gombos et al., 2022), also plays an important role in the fine-tuning of the plant DDR. Finally, a large set of DDR and cell-cycle related genes, among which *WEE1*, were upregulated in the *pol2a* background, even in the absence of both E2FB and SOG1 (class C genes), although SOG1 was required for the full induction of their expression, suggesting the involvement of a third partner, likely E2FA (Figure 7B). Importantly, this redundant role of E2FA and E2FB in the regulation of DDR genes likely extends beyond SOG1 targets, as we observed that a large number of cell cycle genes are E2F targets, and remain highly expressed in the absence of both SOG1 and E2FB, strongly suggesting that E2FA is also capable to activate them.

Our observations are reminiscent of the function of E2Fs during the replication stress response in mammalian cells. Indeed, in the absence of replication stress, a negative feedback loop between the repressor E2F6, which accumulates in late S, and activating E2Fs, promotes the expression of E2F targets involved in DNA synthesis such as PCNA (Pennycook et al., 2020). In response to replication stress, the checkpoint kinase Chk1 phosphorylates and inhibits E2F6 (Bertoli et al., 2013), which allows activating E2Fs to promote the expression of major replication, repair and checkpoint effectors (Bertoli et al., 2016). This mechanism likely avoids an excessive delay in S-phase progression and accumulation of DNA damage due to fork collapse. Although our observations point to a critical role of E2FB in the control of the G2/M transition after replication stress, we cannot rule out that it could also be required to allow S-phase progression despite replication stress. Such a hypothesis would match the observation that the increase in the proportion of EdU-labeled cells during cumulative EdU experiments was extremely slow in *e2fb-1 pol2a sog1* triple mutants. Thus, besides its likely role in the control of the G2/M transition, E2FB could also function as a positive regulator of fork progression, and its loss of function might aggravate the replication defects of *pol2a* mutants.

## Emerging roles of E2FA and E2FB in the plant DNA damage response

Together, our results point to a unique role of E2FB in the plant cell's response to replication stress. Interestingly, there is accumulating evidence that plant E2Fs are involved in the maintenance of genome integrity and play essential roles in several aspects of the DDR and even DNA repair, consistent with the functions of their animal counterpart. Indeed, both E2FA (Lang et al., 2021) and RBR1 form foci at DSBs and function independently of SOG1 to

promote their repair, likely through their ability to interact with DNA repair proteins (Biedermann et al., 2017; Horvath et al., 2017). In addition, genome-wide identification of target genes revealed that RBR1 controls a large set of DDR genes (Bouyer et al., 2018), suggesting that E2F–RBR1 complexes may both control the expression of DDR genes and directly contribute to DNA repair. The respective roles of E2FA/B in the cellular response to DSBs are beginning to be unraveled, and both factors seem to contribute, E2FA by promoting DNA repair (Biedermann et al., 2017; Horvath et al., 2017), and E2FB possibly by triggering cell cycle arrest, although the two *e2fb-1* alleles do not affect this process in the same way (Lang et al., 2021). Conversely, our results suggest that E2FB is more prominently involved in the cellular response to replication stress in parallel to SOG1, and that E2FA plays only a minor role, possibly because E2FB can substitute for its activity. Only in the absence of E2FB did the *e2fa* mutation trigger sensitivity to replication stress, correlated with a longer S-phase and cell cycle duration that depended on SOG1 activity. Recently, E2FA and E2FB were shown to play distinct roles in the UV-B response (Gómez et al., 2022), as previously shown for E2FC (Gómez et al., 2019). It is therefore likely that plants E2Fs are involved in many aspects of the DDR to promote genome integrity and avoid complete cell cycle arrest triggered by DNA stress. Our transcriptome analysis reveals the extreme complexity of the transcriptional networks involving E2Fs in response to replication stress. We have only scratched the surface of the process, but more refined studies in the future will be required to understand the sequence of events occurring at the gene expression level, and how the interplay between E2FA, E2FB, SOG1 and potentially other E2F family members allows the exquisite regulation of cell cycle and DNA repair genes to maintain growth without compromising genomic integrity.

## Material and methods

### Plant material and growth conditions

All *Arabidopsis thaliana* mutant lines used in this study are in the Columbia-0 (Col-0) background and have been described previously: *e2fa-1* (*MPIZ_244*), *e2fa-2 (GABI-348E09)*, *e2fb-1 (SALK_103138)* and *e2fb-2 (SALK_120959)* mutants were first described in Berckmans et al. (2011a, 2011b). Except for analysis of *WEE1* promoter activity, the *sog1-1* mutant was isolated in the L*er* background (Yoshiyama et al., 2009) but later introgressed in the Col-0 background and was a kind gift of Anne Britt. The *sog1-101* allele was described in Ogita et al.

(2018). The *pol2a-4* mutant has been described in Yin et al. (2009) and further characterized in Pedroza-Garcia et al. (2017).

Seed were sterilized using 5 mL bayrochlore$^{TM}$ and 45 µL of absolute ethanol for 7 min, then washed three times with sterile water and kept at 4°C for 2 days. Seeds were sown on commercially available 0.5× Murashige and Skoog (MS, Duchefa) medium solidified with 0.8% agar (Phyto-Agar HP696, Kalys). Then, plates were transferred to long days (16-h light, 8-h dark, Lumilux Cool White lm, 50 to 70 µmol $m^{-2}$ $s^{-1}$, 21°C) in an *in-vitro* growth chamber. After 2 weeks, plantlets were transferred to soil, kept in short day conditions (8-h light at 20°C, 16-h dark at 18°C) for a week and then transferred to a long-day growth chamber (16-h light, 8-h dark, 21°C).

**Generation of reporter lines**

To construct the transcriptional reporter *pWEE1-GUS,* the full-length promoter region of the *WEE1* gene was PCR-amplified (593 bp upstream of the translational start codon) and cloned into the pDONRP4-P1R entry vector by Gateway BP reaction. Site-directed mutagenesis was carried out to mutate the E2F-binding site GCGCGCAA at the -75 bp position to AACACTGT. Subsequently, both the WT (*pWEE1-FL*) and mutated (*pWEE1-mE2F*) promoter were transferred into the pMK7S*NFm14GW,0 destination vector by Gateway LR reaction. Both constructs were transferred into the *Agrobacterium tumefaciens* C58C1RifR strain harboring the pMP90 plasmid. The obtained Agrobacterium strains were used to generate stably transformed Arabidopsis lines with the floral dip transformation method (Clough and Bent, 1998).

**Root growth assay**

Seeds were germinated on 0.5x MS medium and after 4 days, seedlings were transferred to fresh plates of 0.5x MS medium or 0.5x MS supplemented with 1 mM hydroxyurea (HU). Plates were kept in a vertical position for about 2 weeks under long-day conditions. After 10 weeks, plates were scanned and images were used to measured root length by Fiji software (https://imagej.net/Fiji).

**Flow cytometry**

Flow cytometry was done on flower buds of *e2f* combination mutants. Flowers buds were chopped with the help of a razor blade. Then 1 mL of nuclei isolation buffer (45 mM $MgCl_2$, 30 mM sodium citrate, 60 mM MOPS, 1% (w/v) polyvinylpyrrolidone 10,000 pH 7.2),

containing 0.1% (w/v) Triton X-100, and supplemented with 5 mM sodium metabisulphite and RNAse (5 U/mL). The solution was filtered and propidium iodide was added to the solution to a final concentration of 50 µg/mL. The DNA content of 5,000 to 10,000 stained nuclei was determined using a Cyflow SL3 flow cytometer (Partec-Sysmex) with a 532-nm solid-state laser (30 mW) excitation and an emission collected after a 590-nm long-pass filter. For cell cycle analysis, we used the algorithm available in the FloMax software (flomax.software.informer.com).

**EdU labeling**

Seeds were germinated on 0.5x MS medium and five-day-old seedlings were transferred to 0.5x MS medium supplemented with 10 µM EdU for 30 min. We next performed a Thymidine chase by transferring plantlets to 0.5x MS medium supplemented with an excess concentration of thymidine (100µM). Plantlets were fixed after the 30min EdU pulse, of after a 4h30 chase with 4% (w/v) paraformaldehyde (PFA) dissolved in PME buffer (50 mM PIPES pH 6.9, 5 mM $MgSO_4$, 1 mM EGTA) for 15 min under vacuum. After that, plantlets were washed twice with PME to remove the traces of PFA. Squares were drawn on polysine slides using a hydrophobic marker, root tips were cut in a drop of PME under a stereomicroscope. The PME solution was then replaced by an enzyme solution (1% (w/v) cellulase, 0.5% (w/v) cytohelicase, 1% (w/v) pectolyase in PME), and samples were incubated for 1 h in a humid chamber at 37°C. Root tips were then washed three times with 1x PME. After removing most of the liquid, root tips were squashed under a coverslip. Slides were immersed in liquid nitrogen for about 15 s, after which the coverslip was carefully removed. Slides were dried overnight. The next day, slides were washed with 1x PBS (Phosphate Buffer Saline, Sigma) and then with 3% BSA (w/v) prepared in 1x PBS. Samples were permeabilized in 0.5% Triton dissolved in 1x PBS for 30 min. Slides were washed twice with 3% BSA+1x PBS, and then the samples were incubated with Click-iT Plus EdU Alexa Fluor 488 Imaging Kit (Thermo Fisher Scientific) according to the manufacturer's instructions, for 30 min in the dark at room temperature. Once washed with PBS 1x (pH 7.4) + BSA 3%, the nuclei were stained with Hoechst 33342 (1 µg/mL). Slides were mounted in Vectashield® and observed using an epifluorescence microscope equipped with an Apotome module (AxioImager Z.2; Carl Zeiss) fitted with a metal halide lamp and the appropriate filter sets for imaging DAPI and Alexa 488 dyes. Images were acquired with a cooled CCD camera (AxioCam 506 monochrome; Carl Zeiss) operated using the Zen Blue software (Carl Zeiss).

**Meristem length measurement**

For measuring the apical root meristem, 7-day-old root tips were stained with 10 µM PI for about 5 min, and then observed with a Zeiss LSM 880 laser scanning confocal microscope using a 561-nm laser for excitation. Fluorescence was acquired between 470 nm and 700 nm. Representative images were collected from 10 to 15 roots with three biological replicates. Meristem length was estimated by measuring the distance from the quiescent center to the first elongating cell in the cortex cell file.

**GUS staining**

For GUS staining, whole seedlings were stained in a 6-well plate (Falcon 3046; Becton Dickinson) as described (Beeckman and Engler, 1994). Briefly, plants were fixed in an ice-cold 80% (v/v) acetone solution for 30 min. Samples were washed three times with phosphate buffer (14 mM $NaH_2PO_4$ and 36 mM $Na_2HPO_4$) before being incubated in staining buffer (0.5 mg/mL 5-bromo-4-chloro-3-indolyl-b-D-glucuronic acid, 0.165 mg/mL potassium ferricyanide, 0.211 mg/mL potassium ferrocyanide, 0.585 mg/mL EDTA pH8, and 0.1% (v/v) Triton-X100, dissolved in phosphate buffer) at 37°C for 1 h. Samples mounted in lactic acid were observed and photographed with a stereomicroscope (Olympus BX51 microscope).

**RNA extraction, RNA-Seq library preparation and quantitative RT-PCR**

For RNA-Seq on shoot apices, total RNAs were extracted from the shoot apex (first 2 leaves and meristematic zone) of 30 seven-day-old plantlets, using the RNA-Plus kit (Macherey-Nagel), and libraries were prepared with 1µg of total RNA using the NEBNext® Ultra™ II RNA Library Prep Kit for Illumina® according to the manufacturer's instructions. For RNA-Seq experiments performed on root tips, the first 2 mm of 7-day-old seedlings were collected in liquid nitrogen. RNA from samples was extracted using the RNeasy Plant Mini kit (QIAGEN) and cDNA was prepared from 1 µg of RNA using the iScript cDNA synthesis kit (Bio-Rad), both according to the manufacturer's protocols. Libraries were sequenced on a HiSeq2000 or NextSeq500 75-bp single-end run.

Quantitative RT-PCR was performed in a final volume of 5 µl with SYBR Green I Master (Roche) and analyzed with a Lightcycler 480 (Roche) or LC96 (Roche). For each reaction, three biological and three technical repeats were performed. Primers used in this study are listed in Table S9.

**RNA-Seq data analysis**

Single-end sequencing of RNA-Seq samples were trimmed using Trimmomatic-0.38 (Bolger et al., 2014) with the parameters: Minimum length of 30 bp; Mean Phred quality score greater than 30; Leading and trailing bases removal with base quality <5. Bowtie2 aligner (Langmead and Salzberg, 2012) was used for mapping to TAIR11 genome assembly. Raw read counts were used to identify differentially expressed genes using the DiCoExpress package (Lambert et al., 2020).

**Chromatin immunoprecipitation followed by high-throughput sequencing (ChIP-seq) assay**

ChIP-seq was done on 2-week-old plantlets expressing the E2FB-GFP fusion. Plantlets were crosslinked in 1 % (v/v) of formaldehyde for 15 min. Crosslinking was then quenched with 125 mM glycine for 5 min. Crosslinked plantlets were grounded in liquid nitrogen and nuclei were isolated in Nuclei Lysis Buffer (0.1% SDS, 50 mm Tris-HCl pH 8, 10 mm ethylene diamine tetra acetic acid EDTA pH 8). Chromatin was sonicated for 7 min using Covaris S220 (Peak Power: 175, cycles/burst: 200. Duty Factory: 20). The sonicated chromatin was then immuno-precipitated using anti GFP antibodies (abcam, ab290), incubated at 4°C overnight with rotation on a rotating wheel. Immunocomplexes were recovered with 40 µL of Dynabeads protein A (Invitrogen, 10002D) and incubated for 2 h at 4°C with rotation. Immunoprecitated material was washed 6 times for 5 min with ChIP dilution buffer (1.1% Triton X-100, 1.2 mM EDTA, 16.7 mM Tris-HCl pH8, 167 mM NaCl, protease inhibitors) and twice in TE (1 mm Tris-HCl pH 8, 1 mM EDTA pH 8). ChIPed DNA was eluted by two 15-min incubations at 65°C with 200 µL of freshly prepared elution buffer (1% SDS, 0.1 m $NaHCO_3$). Chromatin was reverse crosslinked by adding 16 µL of 5 M NaCl, incubated overnight at 65°C. The next day, chromatin was treated with RNase and Proteinase K, incubated for 3 h at 50°C, and DNA was extracted with phenol-chloroform. Ethanol was used to precipitate DNA in the presence of glycoblue and was then resuspended in 10 µL of nuclease free water. Libraries were then generated using 10 ng of DNA with NEBNext Ultra II DNA Library Prep Kit for Illumina (NEB). The quality of the libraries was assessed with Agilent 2100 Bioanalyzer Instrument, and the libraries were subjected to $1 \times 7$ bp high-throughput sequencing by NextSeq 500 (Illumina).

**Statistical analysis**

Statistical analyses were performed as indicated in the figure legends.

**Data availability**

RNA-Seq raw data from this study were deposited in Gene Expression Omnibus (accession number GSE220849 for RNAseq data obtained on root tips of *e2fa-2 e2fb-1* mutants, and GSE220872 for transcriptome data obtained in *pol2a*, *e2fb-1 pol2a* and *e2fb-1 pol2a sog1* mutants). Analysis of ChIP-seq raw data is described in more details in (Gombos et al., 2022), but raw data is available in Gene Expression Omnibus (accession number GSE218481). Sequence data from this article can be found in the Arabidopsis Genome Initiative or GenBank/EMBL databases under the following accession numbers: *E2FA* (At2g36010); *E2FB* (At5g22220); *POL2A* (AT1G08260); *SOG1*(AT1g25580).

**Supplemental data**

The following materials are available in the online version of this article.

**Supplemental Figure S1: Cumulative EdU incorporation suggests that cell cycle progression is extremely slow in *e2fb-1 pol2a sog1* mutants.**

**Supplemental Figure S2: Loss of E2FB but not E2FA affects cell cycle progression in flower buds of *pol2a* or *pol2a sog1* mutants.**

**Supplemental Figure S3: SOG1 targets that are negatively regulated by E2FB are not repressed by E2FA**

**Supplemental Figure S4: Expression of *ANAC044* and *ANAC085* is under the control of SOG1 and E2FA/E2FB.**

**Supplemental Figure S5: Genes specifically up-regulated in *pol2a sog1* and *e2fb-1 pol2a sog1* are enriched in cell cycle-related genes and E2Fa targets.**

**Supplemental Figure S6: Representative pictures of plantlets grown on control medium (MS) or medium supllemented with HU (1mM) used to obtain the data shown on Figure 6.**

**Supplemental Figure S7: *e2fa-2 e2fb-1 sog1* triple mutants are hypersensitive to replication stress.**

**Supplemental Figure S8. The *e2fa-2 e2fb-1* double knockout but not single mutants, tends to have fewer cells in root meristems and longer S-phase.**

**Supplemental Table S1: List of E2FA (S1A), E2FB (S1B) targets and their shared targets with SOG1 (S1C).**

**Supplemental Table S2: DEG in *pol2a, pol2a sog1* and *e2fb-1-1 pol2a sog1* mutants**

**Supplemental Table S3: Overlaps between up-regulated genes in the analyzed mutants**

**Supplemental Table S4: List of genes found in each group shown on Figure 5C.**

**Supplemental Table S5: List of DEG identified in the RNA-seq analysis performed on root tips of *e2fa-2 e2fb-1* double mutants: upregulated genes (Table S5A), downregulated genes (Table S5B) and list of upregulated genes targeted by E2FA and/or B (Table S5C).**

**Supplemental Table S6: List of DNA-replication-related genes down-regulated in *e2fa-2 e2fb-1* double mutants**

**Supplemental Table S7: GO analysis of down-regulated genes in *e2fa-2 e2fb-1* double mutants**

**Supplemental Table S8: GO analysis of up-regulated genes in *e2fa-2 e2fb-1* double mutants**

**Supplemental Table S9: Sequence of primers used in this study**

## Author contributions

L.D.V., M.B. and C.R conceived and designed the research. M.N., C.B., J.A.P.G., C.M., I.V., T.C., J. D.W., R.B.C., T.E., I.V., L.C. and D.L. performed the experiments. M.N., T.E, X.H., Cl.B, Ca.B., K.V, M.B. L.D.V and C.R. analyzed data. L.D.V., M.B. and C.R. wrote the article. All authors read, revised, and approved the article.

## Acknowledgments

The authors thank Etienne Delannoy at Marie-Laure Martin-Magniette (IPS2) for advice on RNA-Seq data analysis; and Annick Bleys for critical reading and editing of the manuscript. Imaging experiments conducted at IPS2 benefited from the Imaging Facility of the Institute.

## Funding

This work was supported by grants of the Research Foundation Flanders (G011420N) and Agence Nationale de la Recherche (21-CE20-0027).

## References

**Beeckman, T., and Engler, G.** (1994). An easy technique for the clearing of histochemically stained plan tissue. *Plant Mol. Biol. Report.* **12**:37–42.

**Berckmans, B., Vassileva, V., Schmid, S. P., Maes, S., Parizot, B., Naramoto, S., Magyar, Z., Alvim Kamei, C. L., Koncz, C., Bogre, L., et al.** (2011a). Auxin-dependent cell cycle reactivation through transcriptional regulation of Arabidopsis E2Fa by lateral organ boundary proteins. *Plant Cell* **23**:3671–3683.

**Berckmans, B., Lammens, T., Van Den Daele, H., Magyar, Z., Bögre, L., De Veylder, L., Bogre, L., and De Veylder, L.** (2011b). Light-dependent regulation of DEL1 is determined by the antagonistic action of E2Fb and E2Fc. *Plant Physiol* **157**:1440–1451.

**Bertoli, C., Klier, S., McGowan, C., Wittenberg, C., and De Bruin, R. A. M.** (2013). Chk1 inhibits E2F6 repressor function in response to replication stress to maintain cell-cycle transcription. *Curr. Biol.* **23**:1629–1637.

**Bertoli, C., Herlihy, A. E., Pennycook, B. R., Kriston-Vizi, J., and de Bruin, R. A. M.** (2016). Sustained E2F-Dependent Transcription Is a Key Mechanism to Prevent Replication-Stress-Induced DNA Damage. *Cell Rep.* **15**:1412–1422.

**Biedermann, S., Harashima, H., Chen, P., Heese, M., Bouyer, D., Sofroni, K., and Schnittger, A.** (2017). The retinoblastoma homolog RBR1 mediates localization of the repair protein RAD51 to DNA lesions in *Arabidopsis*. *EMBO J.* **36**:1279–1297.

**Biswas, A. K., and Johnson, D. G.** (2012). Transcriptional and nontranscriptional functions of E2F1 in response to DNA damage. *Cancer Res.* **72**:13–7.

**Bourbousse, C., Vegesna, N., and Law, J. A.** (2018). SOG1 activator and MYB3R repressors regulate a complex DNA damage network in Arabidopsis. *Proc. Natl. Acad. Sci. U. S. A.* **115**:E12453–E12462.

**Bouyer, D., Heese, M., Chen, P., Harashima, H., Roudier, F., Grüttner, C., and Schnittger, A.** (2018). Genome-wide identification of RETINOBLASTOMA RELATED 1 binding sites in Arabidopsis reveals novel DNA damage regulators. *PLOS Genet.* **14**:e1007797.

**Clough, S. J., and Bent, A. F.** (1998). Floral dip: a simplified method for Agrobacterium-mediated transformation of Arabidopsis thaliana. *Plant J* **16**:735–743.

**De Schutter, K., Joubès, J., Cools, T., Verkest, A., Corellou, F., Babiychuk, E., Van Der Schueren, E., Beeckman, T., Kushnir, S. T., Inzé, D., et al.** (2007). Arabidopsis WEE1 kinase controls cell cycle arrest in response to activation of the DNA integrity checkpoint. *Plant Cell* **19**:211–225.

**De Veylder, L., Beeckman, T., Beemster, G. T., de Almeida Engler, J., Ormenese, S.,**

**Maes, S., Naudts, M., Van Der Schueren, E., Jacqmard, A., Engler, G., et al.** (2002). Control of proliferation, endoreduplication and differentiation by the Arabidopsis E2Fa-DPa transcription factor. *EMBO J* **21**:1360–1368.

**del Pozo, J. C., Boniotti, M. B., and Gutierrez, C.** (2002). Arabidopsis E2Fc functions in cell division and is degraded by the ubiquitin-SCF(AtSKP2) pathway in response to light. *Plant Cell* **14**:3057–3071.

**Friesner, J. D., Liu, B., Culligan, K., and Britt, A. B.** (2005). Ionizing radiation-dependent gamma-H2AX focus formation requires ataxia telangiectasia mutated and ataxia telangiectasia mutated and Rad3-related. *Mol Biol Cell* **16**:2566–2576.

**Giangrande, P. H., Zhu, W., Schlisio, S., Sun, X., Mori, S., Gaubatz, S., and Nevins, J. R.** (2004). A role for E2F6 in distinguishing G1/S- and G2/M-specific transcription. *Genes Dev.* **18**:2941–51.

**Gombos, M., Raynaud, C., Nomoto, Y., Molnár, E., Brik-Chaouche, R Takatsuka, H., Zaki, A., Bernula, D., Latrasse, D., Mineta, K., Nagy, F., et al.** (2022). The canonical E2Fs together with RETINOBLASTOMA-RELATED are required to establish quiescence during plant development. *bioRxiv* Advance Access published December 6, 2022, doi:10.1101/2022.12.05.519120.

**Gómez, M. S., Ferreyra, M. L. F., Sheridan, M. L., Casati, P., Falcone Ferreyra, M. L., Sheridan, M. L., and Casati, P.** (2019). Arabidopsis E2Fc is required for the DNA damage response under UV-B radiation epistatically over the microRNA396 and independently of E2Fe **97**:749–764.

**Gómez, M. S., Sheridan, M. L., and Casati, P.** (2022). E2Fb and E2Fa transcription factors independently regulate the DNA damage response after ultraviolet B exposure in Arabidopsis. *Plant J.* **109**:1098–1115.

**Hayashi, K., Hasegawa, J., and Matsunaga, S.** (2013). The boundary of the meristematic and elongation zones in roots: endoreduplication precedes rapid cell expansion. *Sci. Rep.* **3**:2723.

**Heyman, J., Van den Daele, H., De Wit, K., Boudolf, V., Berckmans, B., Verkest, A., Alvim Kamei, C. L., De Jaeger, G., Koncz, C., and De Veylder, L.** (2011). Arabidopsis ULTRAVIOLET-B-INSENSITIVE4 maintains cell division activity by temporal inhibition of the anaphase-promoting complex/cyclosome. *Plant Cell* **23**:4394–4410.

**Horvath, B. M., Kourova, H., Nagy, S., Nemeth, E., Magyar, Z., Papdi, C., Ahmad, Z., Sanchez-Perez, G. F., Perilli, S., Blilou, I., et al.** (2017). Arabidopsis

RETINOBLASTOMA RELATED directly regulates DNA damage responses through functions beyond cell cycle control. *EMBO J.* **36**:1261–1278.

**Hu, Z., Cools, T., Kalhorzadeh, P., Heyman, J., and De Veylder, L.** (2015). Deficiency of the Arabidopsis helicase RTEL1 triggers a SOG1-dependent replication checkpoint in response to DNA cross-links. *Plant Cell* **27**:149–61.

**Ishida, S., Huang, E., Zuzan, H., Spang, R., Leone, G., West, M., and Nevins, J. R.** (2001). Role for E2F in control of both DNA replication and mitotic functions as revealed from DNA microarray analysis. *Mol. Cell. Biol.* **21**:4684–99.

**Lambert, I., Paysant-Le Roux, C., Colella, S., and Martin-Magniette, M.-L.** (2020). DiCoExpress: a tool to process multifactorial RNAseq experiments from quality controls to co-expression analysis through differential analysis based on contrasts inside GLM models. *Plant Methods* **16**:68.

**Lammens, T., Li, J., Leone, G., and De Veylder, L.** (2009). Atypical E2Fs: new players in the E2F transcription factor family. *Trends Cell Biol* **19**:111–118.

**Lang, J., Smetana, O., Sanchez-Calderon, L., Lincker, F., Genestier, J., Schmit, A.-C., Houlné, G., and Chabouté, M.-E.** (2012). Plant γH2AX foci are required for proper DNA DSB repair responses and colocalize with E2F factors. *New Phytol.* **194**:353–363.

**Lang, L., Pettkó-Szandtner, A., Tunçay Elbaşı, H., Takatsuka, H., Nomoto, Y., Zaki, A., Dorokhov, S., De Jaeger, G., Eeckhout, D., Ito, M., et al.** (2021). The DREAM complex represses growth in response to DNA damage in Arabidopsis. *Life Sci. alliance* **4**.

**Leviczky, T., Molnár, E., Papdi, C., Őszi, E., Horváth, G. V., Vizler, C., Nagy, V., Pauk, J., Bögre, L., and Magyar, Z.** (2019). E2FA and E2FB transcription factors coordinate cell proliferation with seed maturation. *Development* **146**.

**Li, X., Cai, W., Liu, Y., Li, H., Fu, L., Liu, Z., Xu, L., Liu, H., Xu, T., and Xiong, Y.** (2017). Differential TOR activation and cell proliferation in Arabidopsis root and shoot apexes. *Proc. Natl. Acad. Sci. U. S. A.* **114**:2765–2770.

**Lin, W. C., Lin, F. T., and Nevins, J. R.** (2001). Selective induction of E2F1 in response to DNA damage, mediated by ATM-dependent phosphorylation. *Genes Dev.* **15**:1833–44.

**Lincker, F., Philipps, G., and Chabouté, M.-E.** (2004). UV-C response of the ribonucleotide reductase large subunit involves both E2F-mediated gene transcriptional regulation and protein subcellular relocalization in tobacco cells. *Nucleic Acids Res.* **32**:1430–8.

**Magyar, Z., Bögre, L., and Ito, M.** (2016). DREAMs make plant cells to cycle or to become

quiescent. *Curr. Opin. Plant Biol.* **34**:100–106.

**Maréchal, A., and Zou, L.** (2013). DNA damage sensing by the ATM and ATR kinases. *Cold Spring Harb. Perspect. Biol.* Advance Access published 2013, doi:10.1101/cshperspect.a012716.

**Mariconti, L., Pellegrini, B., Cantoni, R., Stevens, R., Bergounioux, C., Cella, R., and Albani, D.** (2002). The E2F family of transcription factors from Arabidopsis thaliana. Novel and conserved components of the retinoblastoma/E2F pathway in plants. *J Biol Chem* **277**:9911–9919.

**Mazouzi, A., Velimezi, G., and Loizou, J. I.** (2014). DNA replication stress: Causes, resolution and disease. *Exp. Cell Res.* **329**:85–93.

**Müller, H., Bracken, A. P., Vernell, R., Moroni, M. C., Christians, F., Grassilli, E., Prosperini, E., Vigo, E., Oliner, J. D., and Helin, K.** (2001). E2Fs regulate the expression of genes involved in differentiation, development, proliferation, and apoptosis. *Genes Dev.* **15**:267–85.

**Naouar, N., Vandepoele, K., Lammens, T., Casneuf, T., Zeller, G., van Hummelen, P., Weigel, D., Ratsch, G., Inze, D., Kuiper, M., et al.** (2009). Quantitative RNA expression analysis with Affymetrix Tiling 1.0R arrays identifies new E2F target genes. *Plant J* **57**:184–194.

**Nisa, M.-U., Huang, Y., Benhamed, M., and Raynaud, C.** (2019). The Plant DNA Damage Response: Signaling Pathways Leading to Growth Inhibition and Putative Role in Response to Stress Conditions. *Front. Plant Sci.* **10**:653.

**Nisa, M., Bergis, C., Pedroza-Garcia, J.-A. A., Drouin-Wahbi, J., Mazubert, C., Bergounioux, C., Benhamed, M., and Raynaud, C.** (2021). The plant DNA polymerase theta is essential for the repair of replication-associated DNA damage. *Plant J.* **106**:1197–1207.

**Ogita, N., Okushima, Y., Tokizawa, M., Yamamoto, Y. Y., Tanaka, M., Seki, M., Makita, Y., Matsui, M., Okamoto-Yoshiyama, K., Sakamoto, T., et al.** (2018). Identifying the target genes of SUPPRESSOR OF GAMMA RESPONSE 1, a master transcription factor controlling DNA damage response in Arabidopsis. *Plant J.* **94**:439–453.

**Őszi, E., Papdi, C., Mohammed, B., Pettkó-Szandtner, A., Vaskó-Leviczky, T., Molnár, E., Ampudia, C. G., Khan, S., Lopez-Juez, E., Horváth, B., et al.** (2020). E2FB interacts with RETINOBLASTOMA RELATED and regulates cell proliferation during leaf development. *Plant Physiol.* **182**:(518-533.

**Pedroza-Garcia, J. A., Mazubert, C., Del Olmo, I., Bourge, M., Bounon, R., Tariq, Z., Delannoy, E., Pinero, M., Jarillo, J. A., Bergounioux, C., et al.** (2017). Function of the plant DNA Polymerase epsilon in replicative stress sensing, a genetic analysis. *Plant Physiol.* **173**:1735-1749.

**Pedroza-Garcia, J. A., Xiang, Y., and De Veylder, L.** (2022). Cell cycle checkpoint control in response to DNA damage by environmental stresses. *Plant J.* **109**:490–507.

**Pennycook, B. R., Vesela, E., Peripolli, S., Singh, T., Barr, A. R., Bertoli, C., and de Bruin, R. A. M.** (2020). E2F-dependent transcription determines replication capacity and S phase length. *Nat. Commun.* **11**.

**Preuss, S. B., and Britt, A. B.** (2003). A DNA-damage-induced cell cycle checkpoint in Arabidopsis. *Genetics* **164**:323–334.

**Saldivar, J. C., Cortez, D., and Cimprich, K. A.** (2017). The essential kinase ATR: ensuring faithful duplication of a challenging genome. *Nat. Rev. Mol. Cell Biol.* **18**:622–636.

**Sjogren, C. A., Bolaris, S. C., and Larsen, P. B.** (2015). Aluminum-Dependent Terminal Differentiation of the Arabidopsis Root Tip Is Mediated through an ATR-, ALT2-, and SOG1-Regulated Transcriptional Response. *Plant Cell* **27**:2501–2515.

**Sozzani, R., Maggio, C., Varotto, S., Canova, S., Bergounioux, C., Albani, D., and Cella, R.** (2006). Interplay between Arabidopsis activating factors E2Fb and E2Fa in cell cycle progression and development. *Plant Physiol* **140**:1355–1366.

**Sweeney, P. R., Britt, A. B., and Culligan, K. M.** (2009). The Arabidopsis ATRIP ortholog is required for a programmed response to replication inhibitors. *Plant J.* **60**:518–526.

**Vandepoele, K., Raes, J., De Veylder, L., Rouze, P., Rombauts, S., and Inze, D.** (2002). Genome-wide analysis of core cell cycle genes in Arabidopsis. *Plant Cell* **14**:903–916.

**Vandepoele, K., Vlieghe, K., Florquin, K., Hennig, L., Beemster, G. T., Gruissem, W., Van de Peer, Y., Inze, D., and De Veylder, L.** (2005). Genome-wide identification of potential plant E2F target genes. *Plant Physiol* **139**:316–328.

**Verkest, A., Abeel, T., Heyndrickx, K. S., Van Leene, J., Lanz, C., Van De Slijke, E., De Winne, N., Eeckhout, D., Persiau, G., Van Breusegem, F., et al.** (2014). A Generic Tool for Transcription Factor Target Gene Discovery in Arabidopsis Cell Suspension Cultures Based on Tandem Chromatin Affinity Purification. *Plant Physiol.* **164**:1122–1133.

**Vlieghe, K., Vuylsteke, M., Florquin, K., Rombauts, S., Maes, S., Ormenese, S., Van Hummelen, P., Van de Peer, Y., Inze, D., and De Veylder, L.** (2003). Microarray

analysis of E2Fa-DPa-overexpressing plants uncovers a cross-talking genetic network between DNA replication and nitrogen assimilation. *J. Cell Sci.* **116**:4249–59.

**Yao, X., Yang, H., Zhu, Y., Xue, J., Wang, T., Song, T., Yang, Z., and Wang, S.** (2018). The canonical E2Fs are required for germline development in Arabidopsis. *Front. Plant Sci.* **9**.

**Yin, H., Zhang, X., Liu, J., Wang, Y., He, J., Yang, T., Hong, X., Yang, Q., and Gong, Z.** (2009). Epigenetic regulation, somatic homologous recombination, and abscisic acid signaling are influenced by DNA polymerase epsilon mutation in Arabidopsis. *Plant Cell* **21**:386–402.

**Yoshiyama, K., Conklin, P. A., Huefner, N. D., and Britt, A. B.** (2009). Suppressor of gamma response 1 (SOG1) encodes a putative transcription factor governing multiple responses to DNA damage. *Proc Natl Acad Sci U S A* **106**:12843–12848.

## FIGURE LEGENDS

**Figure 1: E2FA, E2FB and SOG1 share common target genes and independently activate *WEE1***

A: Venn diagram showing the overlap between SOG1 (Bourbousse et al., 2018), E2FA (as defined by the union of targets found by TChAP (Verkest et al., 2014) and by ChIP-seq (Gombos et al., 2022; FDR < 0.05 and enrichment > 2.4) and E2Fb target genes (Gombos et al., 2022; FDR < 0.05, enrichment > 2). Significance of overlap was estimated with Fisher's exact test (total number of loci: 38,194 according to Araport11, Cheng et al., 2017).

B: Heatmaps showing E2FA and SOG1 binding on their common target genes, centered around the SOG1 binding site. SOG1 and E2FA binding sites are at very similar positions on most of their common targets, as illustrated by the metaplot above the heatmap.

C: Heatmaps showing E2FB and SOG1 binding on their common target genes, centered around the SOG1 binding site. SOG1 and E2FB binding sites are at very similar positions on most of their common targets, as illustrated by the metaplot above the heatmap.

D, E: Density plots showing overlap of SOG1 and E2FA (D) or E2FB (E) using hexagonal binning routine on their common target genes. Each dot represents the distance from the peak midpoint to the nearest gene. The *y*-axis shows the location of the E2FA (D) or E2FB (E) peak midpoint compared with gene position, while the *x*-axis indicates the position of the SOG1 peak midpoint relative to the nearest gene. Most dots occur close to the diagonal of the graph, showing that E2FA/B and SOG1 bind neighboring sequences. TSS: transcription start site, TES: transcription end site.

F: Constructs encompassing the full-length (FL) *WEE1* promoter driving the expression of the beta-glucuronidase (*GUS*) gene were introduced into wild-type or *sog1-8* mutants. GUS staining was observed after 24 h of treatment with the replicative stress-inducing drug hydroxyurea (1mM). Staining was drastically reduced but still visible in the *sog1-8* background. When the E2F binding site was deleted (*mE2F*), residual activation was lost, demonstrating that E2Fs can contribute to *WEE1* activation in response to replication stress. Scale bars = 50 μm

**Figure 2: E2FB, but not E2FA, is required for sustained plant growth in response to replication stress.**

A: Representative rosette phenotype of 30-day-old plants of the indicated genotype. Scale bars = 1 cm.

B-C: Quantification of rosette area (B) or root length (C) in the indicated genotypes. Data are mean ± SD from at least 15 (B) or 10 (C) measurements for each line and are representative of two independent experiments. On box plots, the vertical size of the boxes shows the interquartile range, and the whiskers correspond to 1.5x the IQR. The horizontal line corresponds to the median. Individual dots indicate values falling outside of this range. Significant differences from the wild type are determined by one-way ANOVA with post-hoc Tukey HSD. Different letters indicate statistically significant differences (ANOVA and Tukey test $p < 0.05$ for B or $p < 0.01$ for C).

**Figure 3: Loss of E2FB, but not E2FA further reduces root apical meristem length in the *pol2a* background by delaying cell cycle progression**

A: Representative confocal images of 7-day-old root apical meristem of wild type (Col-0), *pol2a*, *sog1*, *pol2a sog1*, *e2fb-1*, *e2fb-1 pol2a*, *e2fb-1 sog1* and *e2fb-1 pol2a sog1*. Cell walls were stained with propidium iodide (PI). Only mutant combinations with the *e2fb-1* mutation are shown, because the *e2fa-1* mutation did not have any effect on the phenotype of *pol2a* or *pol2a sog1* mutants, as shown in panel B. Red arrows indicate the upper limit of the apical root meristem. Bars = 50 µm.

B: Quantification of root meristem length in indicated genotypes (n > 10). On box plots, the vertical size of the boxes shows the interquartile range, and the whiskers correspond to 1.5x the IQR. The horizontal line corresponds to the median. Individual dots indicate values falling outside of this range. Different letters indicate statistically relevant differences (ANOVA followed by Tukey test $p < 0.05$). Data are representative of three independent experiments.

C: Pulse EdU labelling (30 min), was used to estimate the proportion of S-phase cells in the meristems of the indicated genotypes. Measures were done on at least 10 root tips (>500 nuclei per root tip).

D: Mitosis in five-day-old roots of all mutant lines labeled with ethynyl-2'-deoxyuridine (EdU). The boxplot represents the proportion of labeled mitosis in the indicated genotypes after 30 min labelling followed by a thymidine 5h chase. Data represent at least 15 roots and are representative of three independent experiments.

For both panels, the vertical size of the boxes shows the interquartile range, and the whiskers correspond to 1.5x the IQR. The horizontal line corresponds to the median. Individual dots indicate values falling outside of this range. Different letters indicate statistically significant differences (binomial ANOVA followed by Tukey post-hoc test $p<0.01$).

**Figure 4: E2FB and SOG1 cooperate to control replicative stress-induced transcriptional changes**

A: Venn diagram showing the overlap between upregulated genes in *pol2a*, *pol2a sog1* and *e2fb-1 pol2a sog1* compared with wild-type plantlets in the shoot apex. Apices were collected from 7-day-old plantlets by removing cotyledons and hypocotyls.

B: GO-term analysis of genes upregulated in all mutant lines.

C: Graphs showing expression changes (using the z-scores available in Table S4) of the three main categories of SOG1 targets that are mis-regulated in *pol2a*, *pol2a sog1* and *e2fb-1 pol2a sog1* mutants.

D: Overlap between SOG1 target genes and mis-regulated genes in triple mutants compared with *pol2a sog1* double mutants. SOG1 targets are significantly more represented amongst upregulated genes, indicating that E2FB acts as a repressor of these genes.

**Figure 5: Simultaneous loss of E2FA, E2FB and SOG1 abolishes the plant's ability to tolerate replication stress**

Plantlets were germinated on 0.5x MS, and transferred on medium supplemented with 1 mM HU after four days. Root lengths were measured after ten days. Data presented are mean ± SD (n > 20). Significant differences from the wild type are determined by one-way ANOVA with

post-hoc Tukey HSD. Different letters indicate statistically significant differences (ANOVA and Tukey test $p < 0.01$). Representative images of plants are shown on Supplemental Figure S6.

**Figure 6: E2F deficiency triggers replication stress, SOG1-dependent cell cycle delay and activation of DDR genes**

A-B: S-phase (A) and total cell cycle duration (B) were measured using a time course of EdU staining according to the protocol of Hayashi et al. (2013).

C: Overlap between up- and downregulated genes in *e2fa-2 e2fb-1* mutant against experimental dataset of E2FA-bound genes (Verkest et al., 2014 and Gombos et al, 2022).

D-E: Relative expression levels of genes downregulated (B) or upregulated (C) in root tips of 7-day-old wild-type, *e2fa-2 e2fb-1*, *sog1* and *e2fa-2 e2fb-1 sog1* mutant seedlings. Data represent mean ± SEM. Experiment was done in three technical and three biological repeats of at least 100 root tips. Significance was tested with Student's t-test. Means with different letters are significantly different ($p < 0.05$).

**Figure 7: SOG1, E2FA and E2FB act on both distinct and common targets to fine-tune the plant DDR.**

A: Our genetic analysis shows that SOG1 and E2Fs function independently to fine-tune DDR gene expression and allow sustained plant growth in response to replication stress.

B: DDR genes can be distributed amongst three classes. One first set of genes (class A) depends only on SOG1 for their activation. Class B genes are antagonistically regulated by SOG1 and E2FB, suggesting that E2FB could dampen SOG1-dependent cell cycle arrest to avoid complete developmental arrest. Among those, negative regulators of the cell cycle such as ANAC085 and ANAC044 may contribute to the severe cell cycle arrest observed in *e2fb pol2a sog1* triple mutants. Class C genes are also targeted both by SOG1 and E2FA/B, and remain induced at similar levels by replication stress even in the absence of SOG1 and E2FB, suggesting that they are redundantly controlled by both E2FA and E2FB.

Image created with BioRender.com.

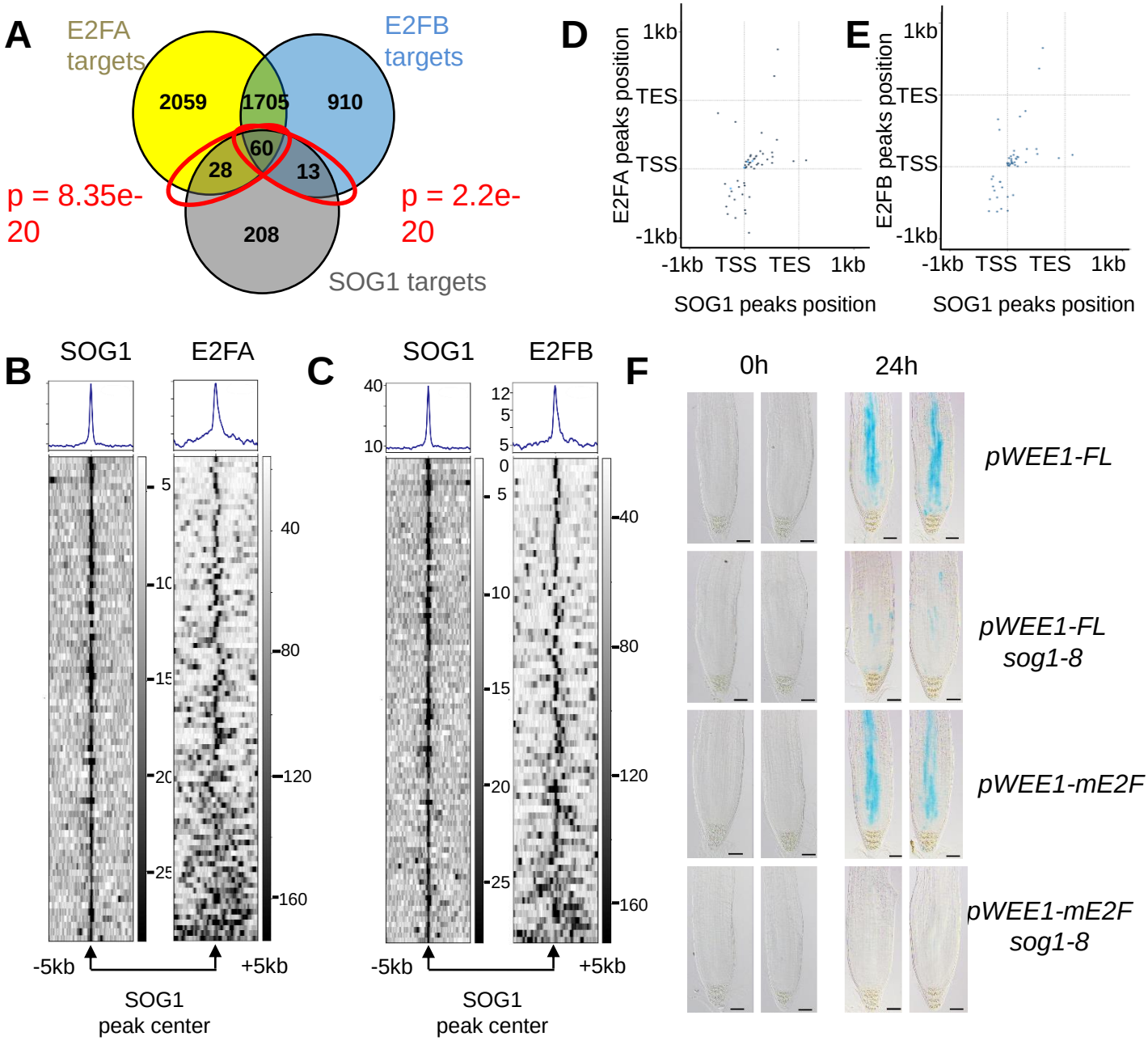
A
E2FA targets
E2FB targets
2059
1705
910
60
28
13
208
SOG1 targets
p = 8.35e-20
p = 2.2e-20
D
E2FA peaks position
1kb
TES
TSS
-1kb
-1kb TSS TES 1kb
SOG1 peaks position
E
E2FB peaks position
1kb
TES
TSS
-1kb
-1kb TSS TES 1kb
SOG1 peaks position
B
SOG1
E2FA
-5kb
+5kb
SOG1
peak center
C
SOG1
E2FB
-5kb
+5kb
SOG1
peak center
F
0h
24h
pWEE1-FL
pWEE1-FL
sog1-8
pWEE1-mE2F
pWEE1-mE2F
sog1-8

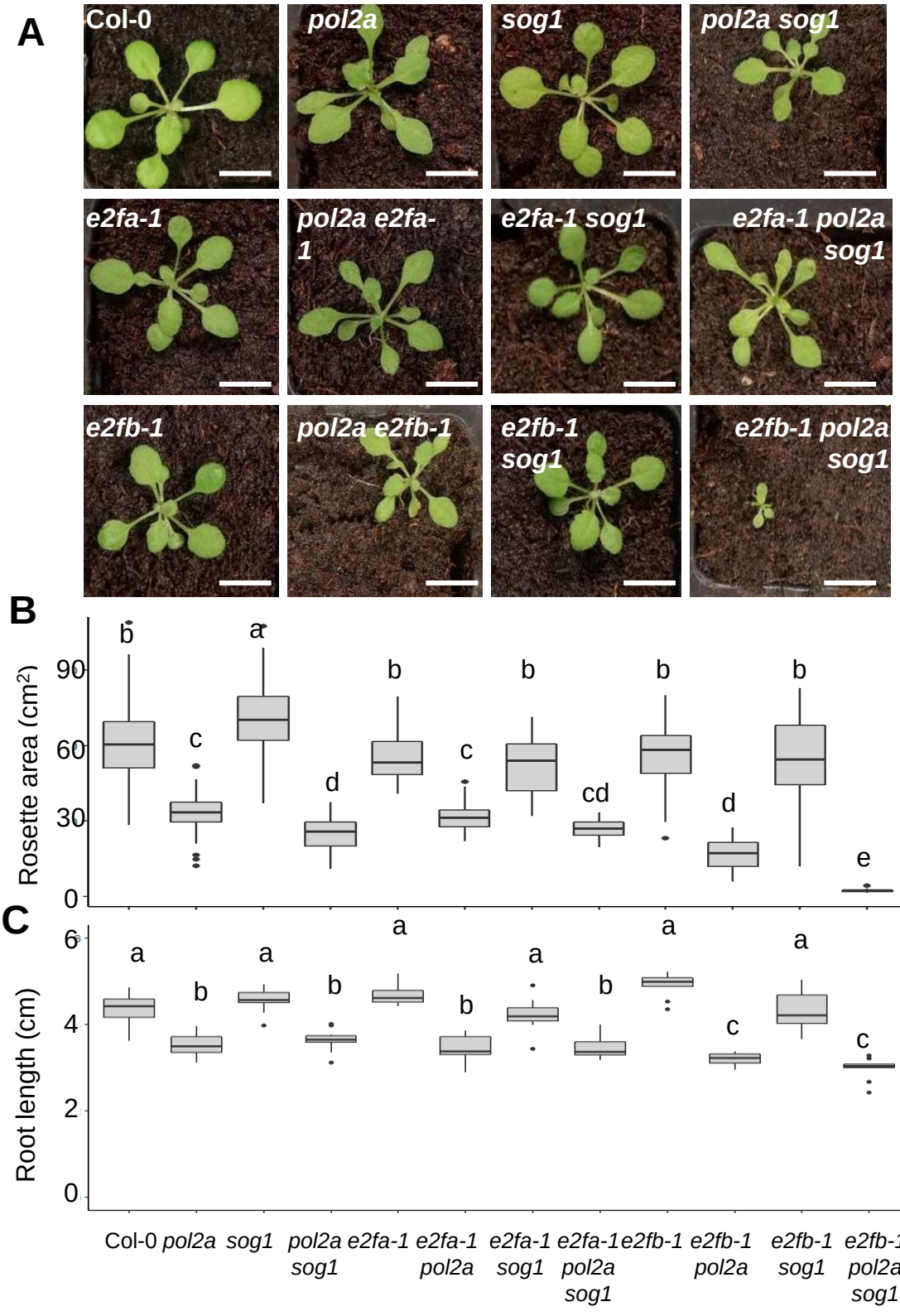
A
Col-0
pol2a
sog1
pol2a sog1
e2fa-1
pol2a e2fa-1
e2fa-1 sog1
e2fa-1 pol2a sog1
e2fb-1
pol2a e2fb-1
e2fb-1 sog1
e2fb-1 pol2a sog1
B
Rosette area (cm²)
0
30
60
90
b
c
a
d
b
c
b
cd
b
d
b
e
C
Root length (cm)
0
2
4
6
a
b
a
b
a
b
a
b
a
c
a
c
Col-0
pol2a
sog1
pol2a sog1
e2fa-1 pol2a
e2fa-1 sog1
e2fa-1 pol2a sog1
e2fb-1
e2fb-1 pol2a
e2fb-1 sog1
e2fb-1 pol2a sog1

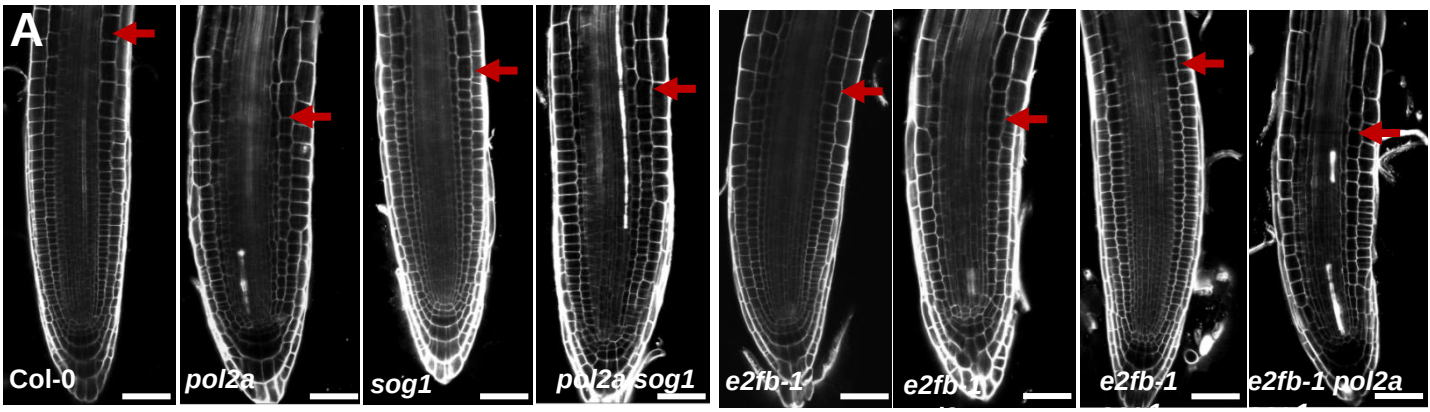
A
Col-0
pol2a
sog1
pol2a sog1
e2fb-1
e2fb-1
e2fb-1
e2fb-1 pol2a

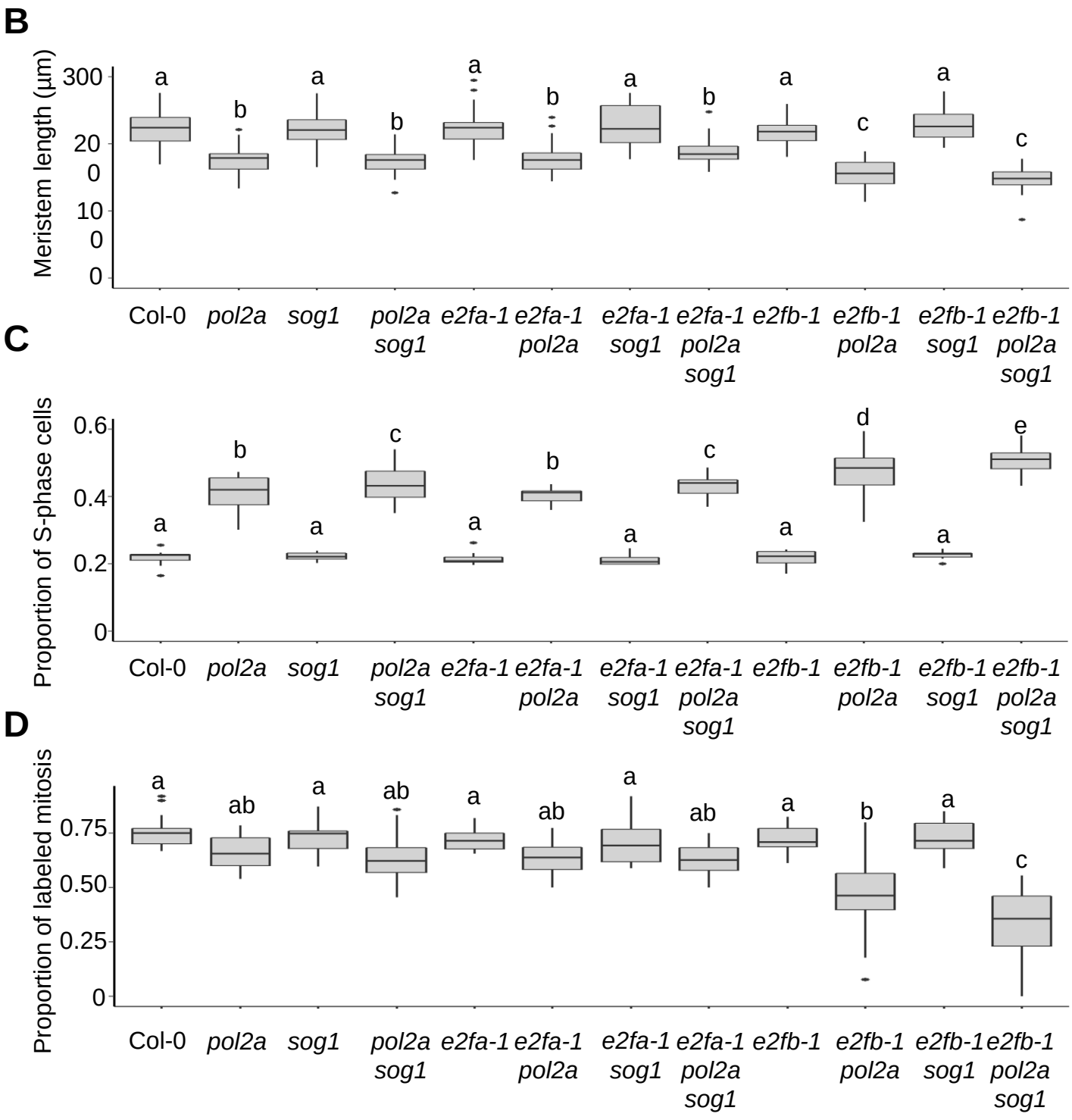
B
Meristem length (µm)
300
20
0
10
0
0
a
b
a
b
a
b
a
b
a
a
c
a
c
Col-0
pol2a
sog1
pol2a sog1
e2fa-1
e2fa-1 pol2a
e2fa-1 sog1
e2fa-1 pol2a sog1
e2fb-1
e2fb-1 pol2a
e2fb-1 sog1
e2fb-1 pol2a sog1
C
Proportion of S-phase cells
0.6
0.4
0.2
0
a
b
a
c
a
b
a
c
a
a
d
a
e
Col-0
pol2a
sog1
pol2a sog1
e2fa-1
e2fa-1 pol2a
e2fa-1 sog1
e2fa-1 pol2a sog1
e2fb-1
e2fb-1 pol2a
e2fb-1 sog1
e2fb-1 pol2a sog1
D
Proportion of labeled mitosis
0.75
0.50
0.25
0
a
ab
a
ab
a
ab
a
ab
a
b
a
c
Col-0
pol2a
sog1
pol2a sog1
e2fa-1
e2fa-1 pol2a
e2fa-1 sog1
e2fa-1 pol2a sog1
e2fb-1
e2fb-1 pol2a
e2fb-1 sog1
e2fb-1 pol2a sog1

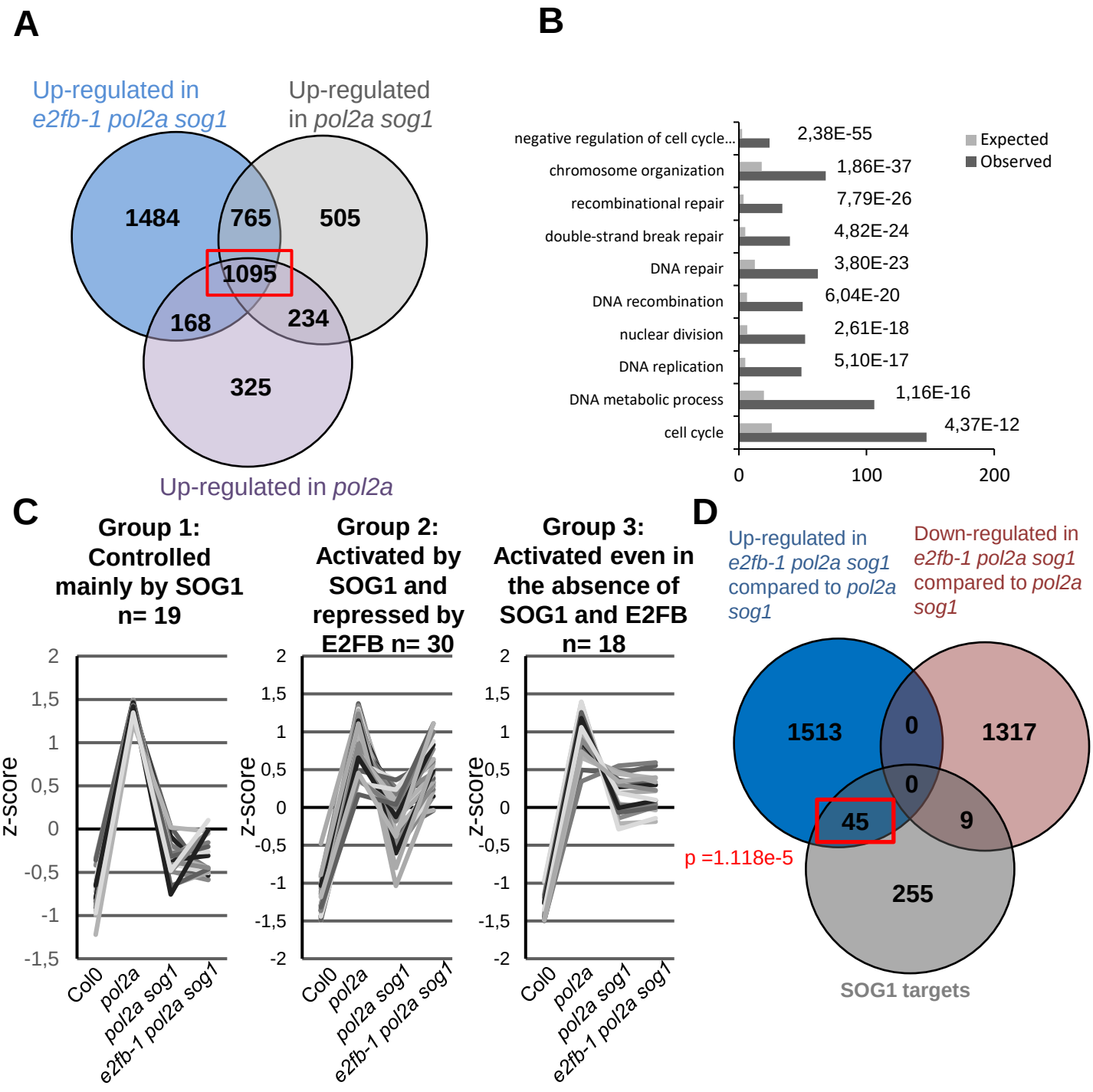
A
Up-regulated in e2fb-1 pol2a sog1
Up-regulated in pol2a sog1
1484
765
505
1095
168
234
325
Up-regulated in pol2a
B
negative regulation of cell cycle...
chromosome organization
recombinational repair
double-strand break repair
DNA repair
DNA recombination
nuclear division
DNA replication
DNA metabolic process
cell cycle
2,38E-55
1,86E-37
7,79E-26
4,82E-24
3,80E-23
6,04E-20
2,61E-18
5,10E-17
1,16E-16
4,37E-12
Expected
Observed
0
100
200
C
Group 1: Controlled mainly by SOG1 n= 19
Group 2: Activated by SOG1 and repressed by E2FB n= 30
Group 3: Activated even in the absence of SOG1 and E2FB n= 18
z-score
Col0
pol2a
pol2a sog1
e2fb-1 pol2a sog1
D
Up-regulated in e2fb-1 pol2a sog1 compared to pol2a sog1
Down-regulated in e2fb-1 pol2a sog1 compared to pol2a sog1
1513
0
1317
0
45
9
255
p =1.118e-5
SOG1 targets

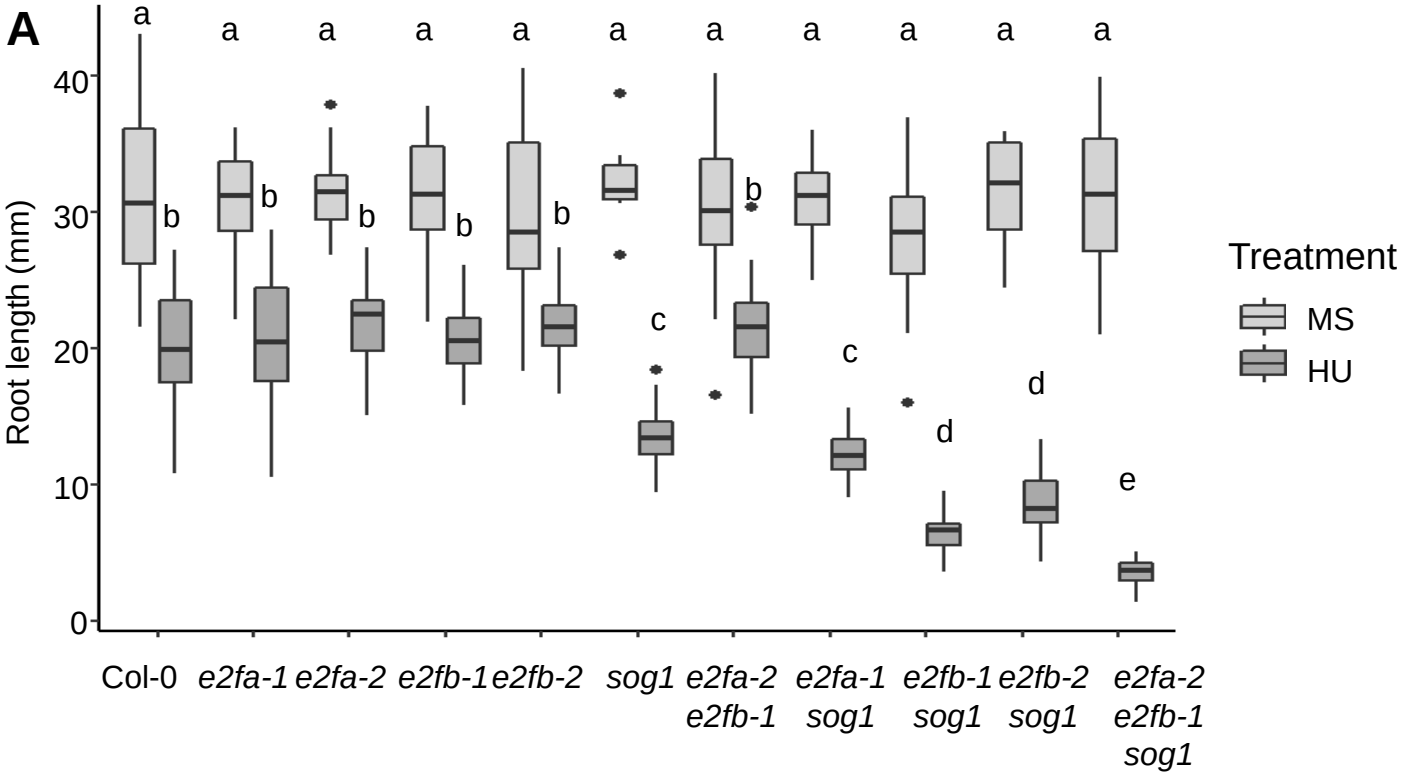
A
Root length (mm)
0
10
20
30
40
a
a
a
a
a
a
a
a
a
a
a
b
b
b
b
b
c
b
c
d
d
e
Col-0
e2fa-1
e2fa-2
e2fb-1
e2fb-2
sog1
e2fa-2 e2fb-1
e2fa-1 sog1
e2fb-1 sog1
e2fb-2 sog1
e2fa-2 e2fb-1 sog1
Treatment
MS
HU

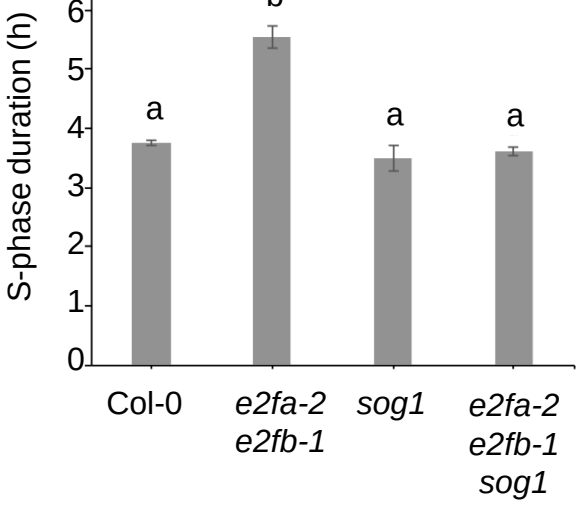
S-phase duration (h)
0
1
2
3
4
5
6
a
b
a
a
Col-0
e2fa-2 e2fb-1
sog1
e2fa-2 e2fb-1 sog1

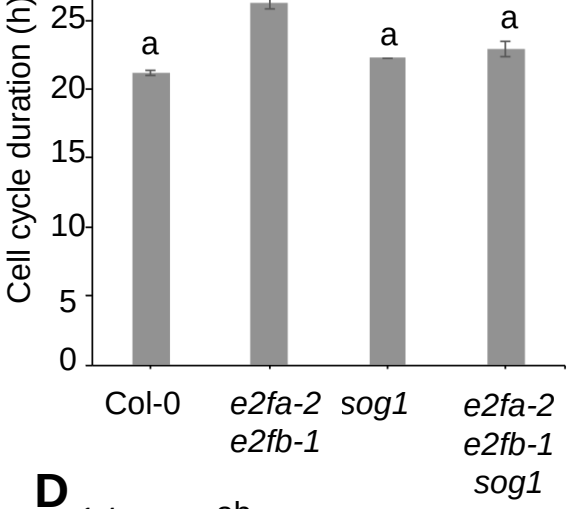
Cell cycle duration (h)
0
5
10
15
20
25
a
a
a
Col-0
e2fa-2 e2fb-1
sog1
e2fa-2 e2fb-1 sog1

C

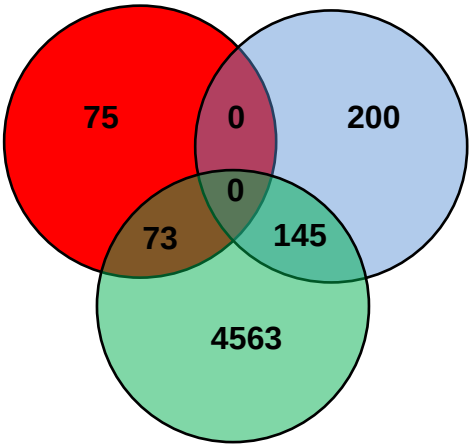
Down in e2fab
Up in e2fab
75
0
200
0
73
145
4563
E2FA and E2FB targets

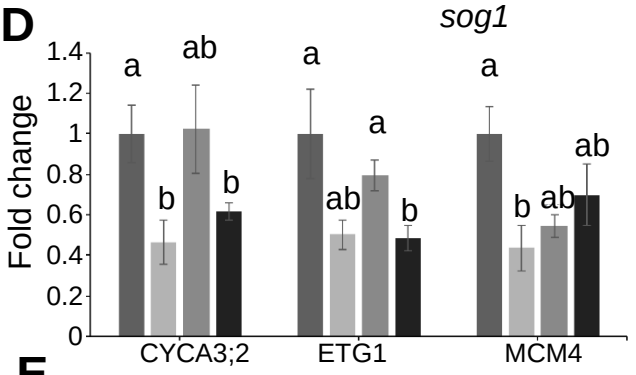
D
Fold change
0
0.2
0.4
0.6
0.8
1
1.2
1.4
a
b
ab
b
a
ab
a
b
a
b
ab
ab
CYCA3;2
ETG1
MCM4

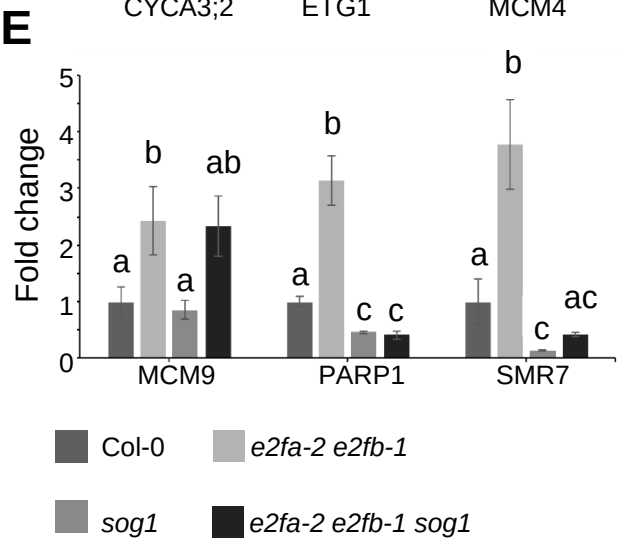
E
Fold change
0
1
2
3
4
5
a
b
a
ab
a
b
c
c
a
b
c
ac
MCM9
PARP1
SMR7
Col-0
e2fa-2 e2fb-1
sog1
e2fa-2 e2fb-1 sog1

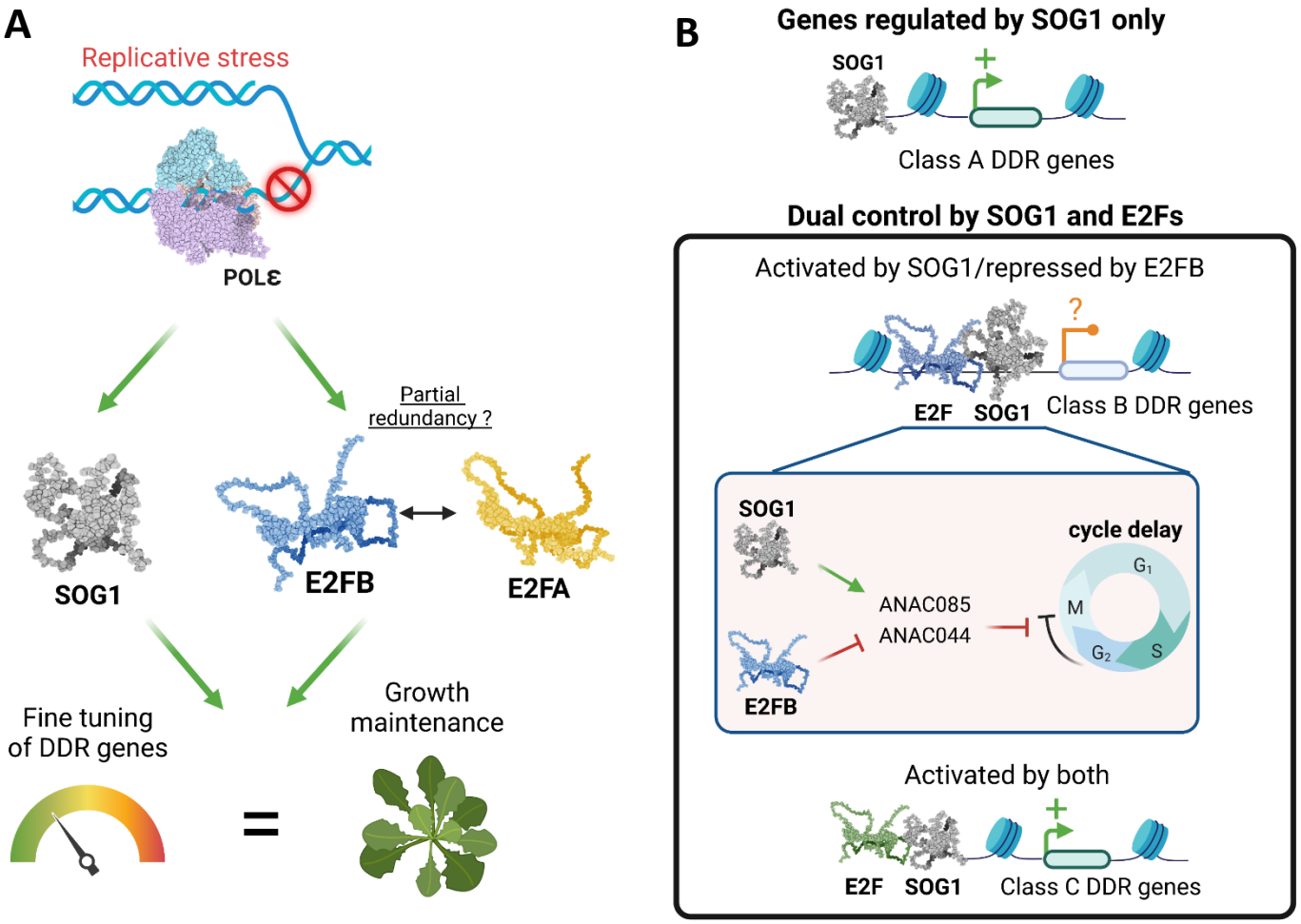
A
Replicative stress
POLε
Partial redundancy ?
SOG1
E2FB
E2FA
Fine tuning of DDR genes
Growth maintenance
=
B
Genes regulated by SOG1 only
SOG1
Class A DDR genes
Dual control by SOG1 and E2Fs
Activated by SOG1/repressed by E2FB
?
E2F
SOG1
Class B DDR genes
SOG1
cycle delay
ANAC085
ANAC044
E2FB
G1
M
G2
S
Activated by both
E2F
SOG1
Class C DDR genes

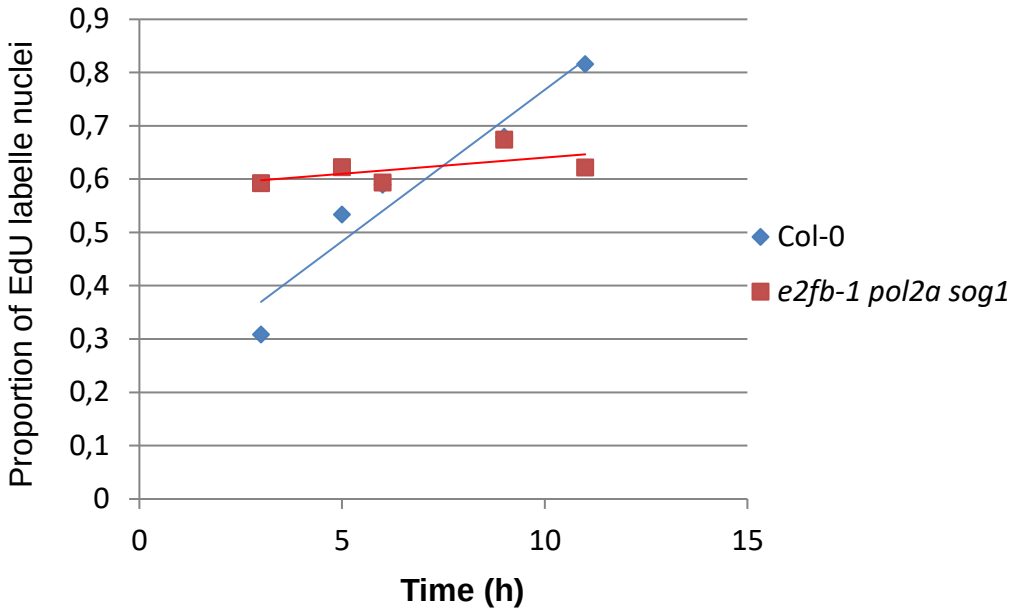


**Supplemental Figure S1: Cumulative EdU incorporation suggests that cell cycle progression is extremely slow in *e2fb-1 pol2a sog1* mutants.**
Cumulative EdU incorporation was performed on wild type (Col-0) and *e2fb-1 pol2a sog1* triple mutants for 12 h. At each timepoint, the proportion of EdU-positive nuclei was estimated through microscopic analysis (n > 1000). The proportion of EdU-labeled nuclei was very high at early timepoints in the triple mutant, indicating that the S-phase duration represents a high proportion of the total cell cycle length. Furthermore, this proportion remained stable throughout the kinetics, indicating that progression through the cell cycle is very slow.

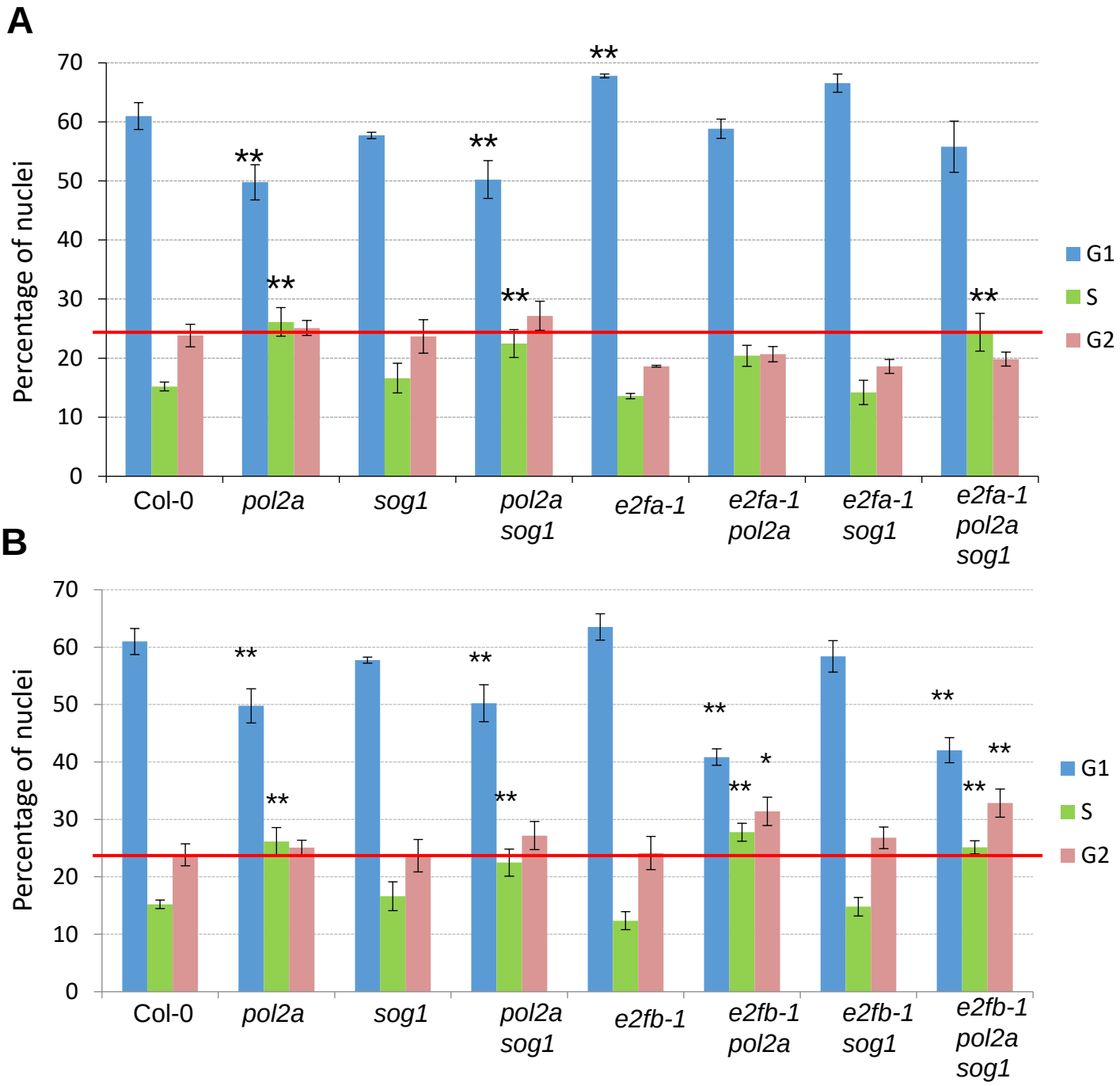


**Supplemental Figure S2: Loss of E2FB but not E2FA affects cell cycle progression in flower buds of *pol2a* or *pol2a sog1* mutants.**

Flow cytometry was used to analyze the cell cycle phases in the flower buds of all mutant lines. For each cell cycle phase, the percentage of nuclei was calculated. Values are average ± SD. Asterisks denote significant differences with respect to percentages observed in the wild type (Kruskal-Wallis test with a Benjamini-Hochberg correction, * $p < 0.05$, ** $p < 0.01$). Data are representative of three biological replicates. The red line indicates the proportion of G2 nuclei in the wild-type.

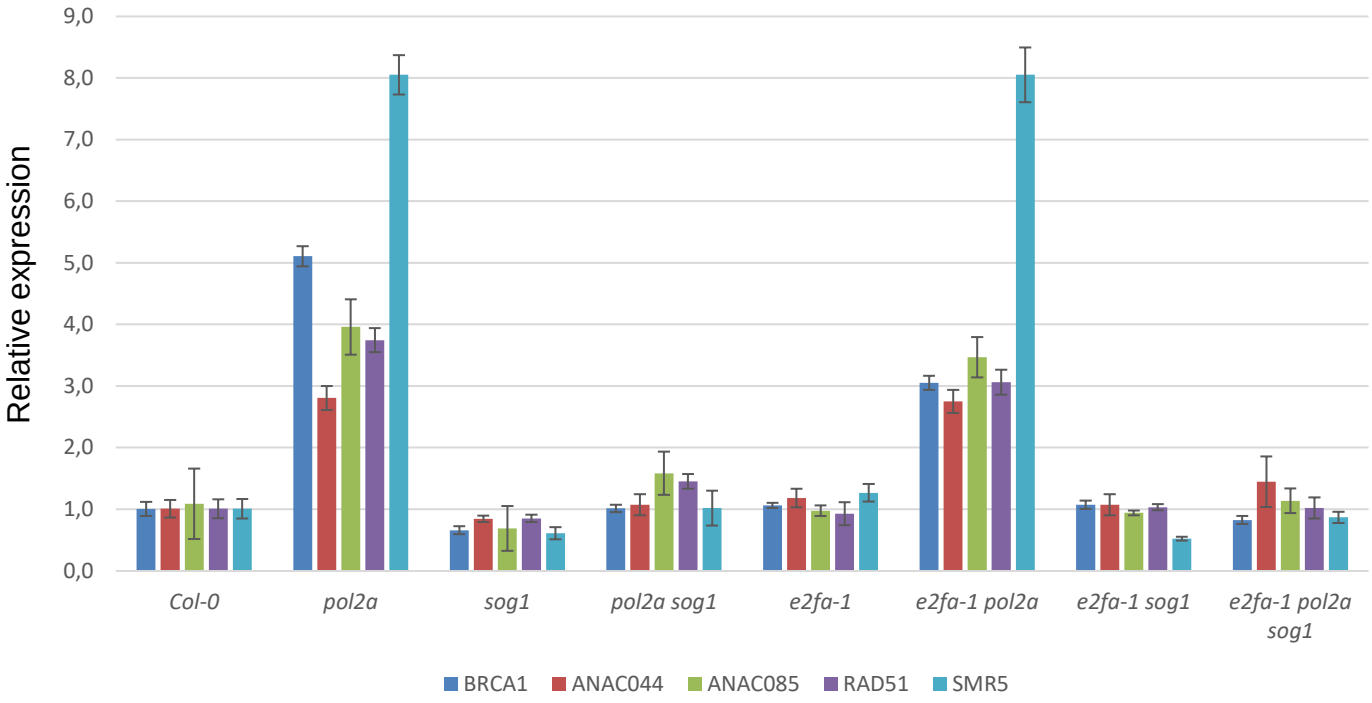


**Supplemental Figure S3: SOG1 targets that are negatively regulated by E2FB are not repressed by E2FA**

Expression of 5 genes that we found to be antagonistically regulated by SOG1 and E2FB was monitored by qRT-PCR in the indicated mutants. As observed in our RNAseq analysis, expression of these genes was reduced in *pol2a sog1* mutants compared to *pol2a* mutants. By contrast, their expression was not affected by the *e2fa-1* mutation: it remained at similar levels in *e2fa-1 pol2a* compared to *pol2a* mutants, and loss of E2FA could not reactivate their expression in the *pol2a sog1* background.

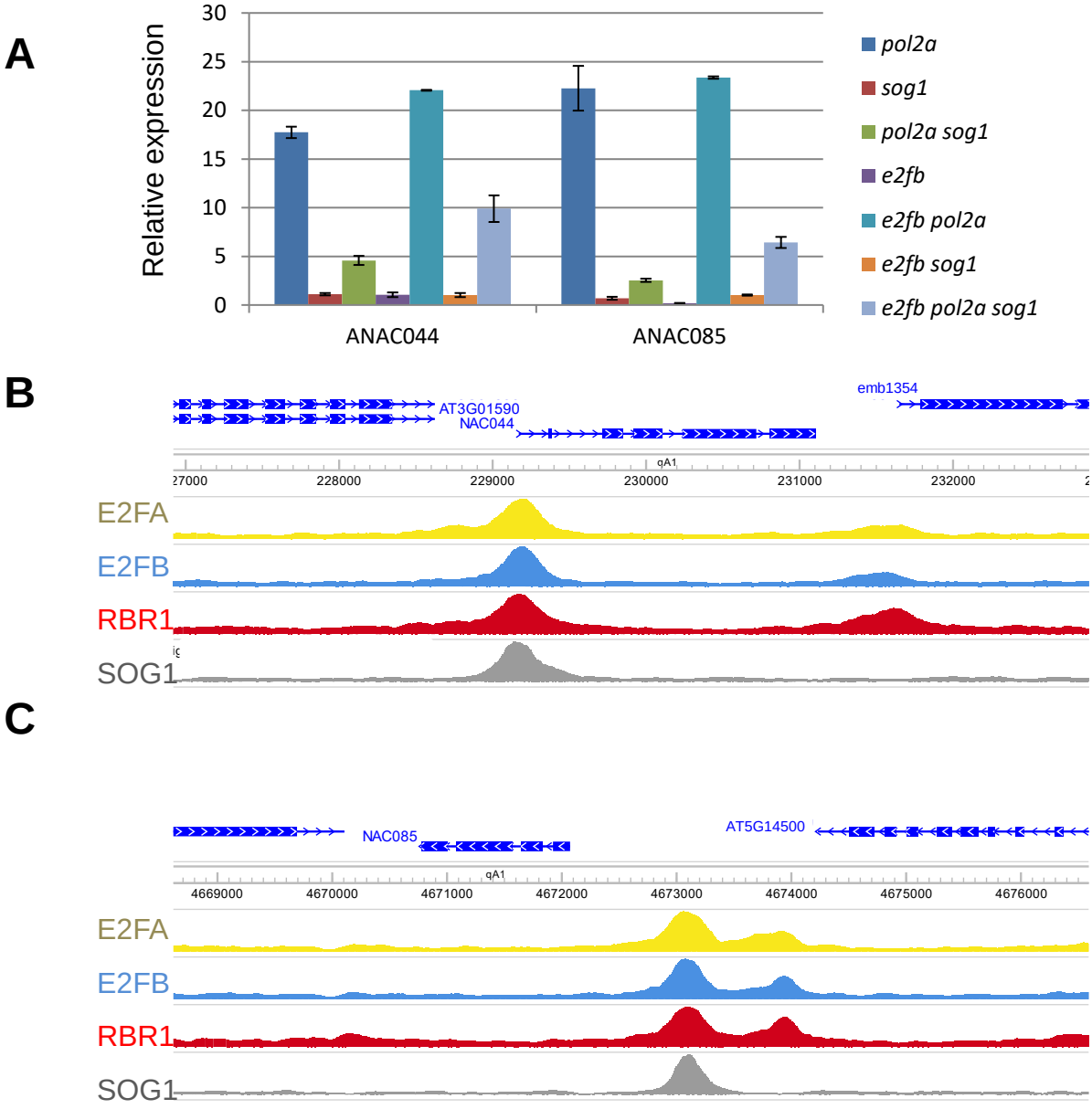


**Supplemental Figure S4: Expression of *ANAC044* and *ANAC085* is under the control of SOG1 and E2FA/B.**

A: RT-qPCR analysis of *ANAC044* and *ANAC085* expression in the indicated mutant lines. RNA was extracted from shoot apices of 5-day-old plantlets. Expression was normalized with the *TIP4* and *SAND* genes as described in Gentric et al. (2020).

B: Screenshot of ChIP-seq data showing E2FA, E2FB, RBR1 and SOG1 binding on the promoter of *ANAC044*.

C: Screenshot of ChIP-seq data showing E2FA, E2FB, RBR1 and SOG1 binding on the promoter of *ANAC085*.

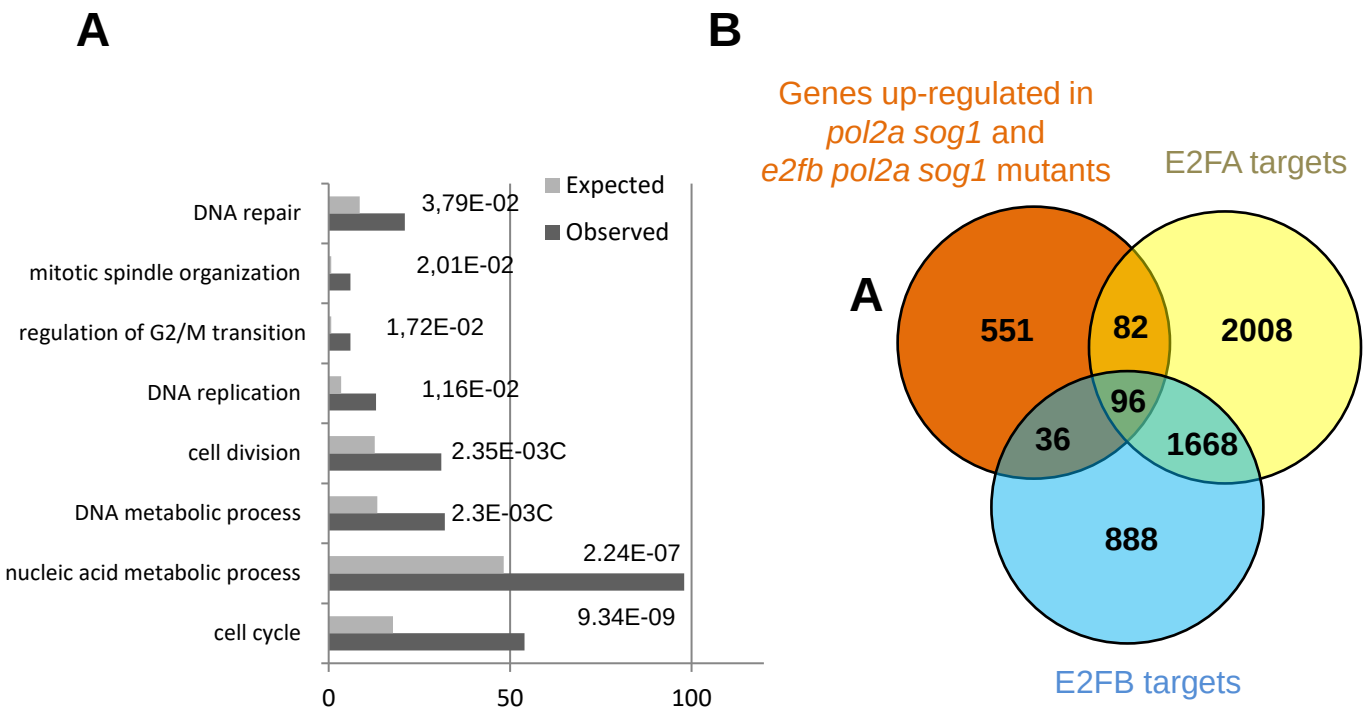


**Supplemental Figure S5: Genes specifically upregulated in *pol2a sog1* and *e2fb-1 pol2a sog1* are enriched in cell cycle-related genes and E2Fa targets.**

A: GO analysis of the 765 genes upregulated in *pol2a sog1* and *e2fb pol2a sog1* but not in *pol2a* mutants.

B: Overlap between this list of genes and the list of E2FA and E2FB target genes. E2FA and E2FB targets were significantly enriched amongst genes upregulated in pol2a sog1 and in e2fb-1 pol2a sog1 ($p = 3.365e-04$ and $p = 1.734e-05$ respectively, Fisher's exact test, total number of genes detected in the RNA-Seq analysis = 20,946).

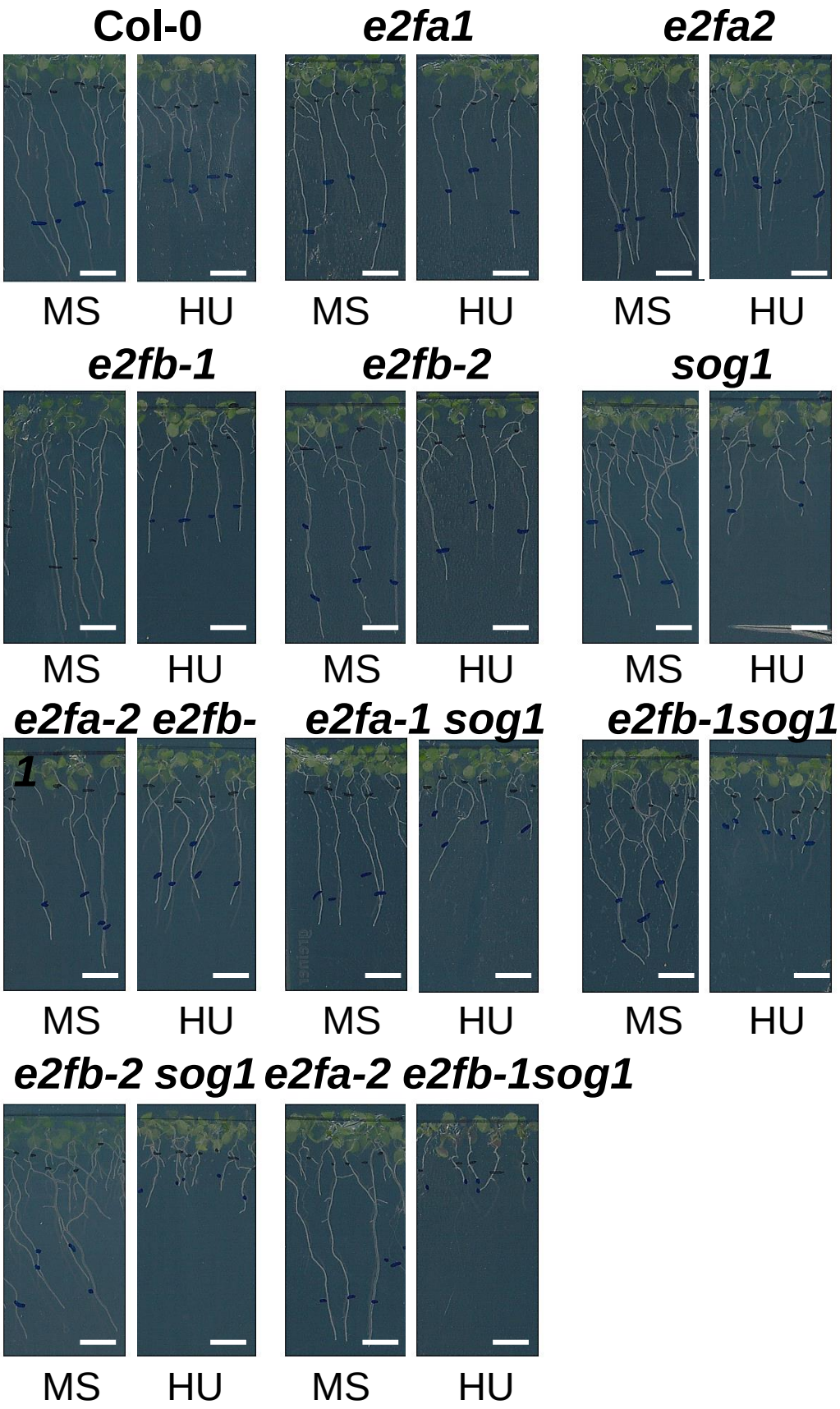


**Supplemental Figure S6. Representative pictures of plantlets grown on control medium (MS) or medium supllemented with HU (1mM) used to obtain the data shown on Figure 6.** Plants were grown on control medium for 4 days, and transferred to control or HU supplemented medium, and grown vertically for 8 days. Bar = 1 cm for all panels.

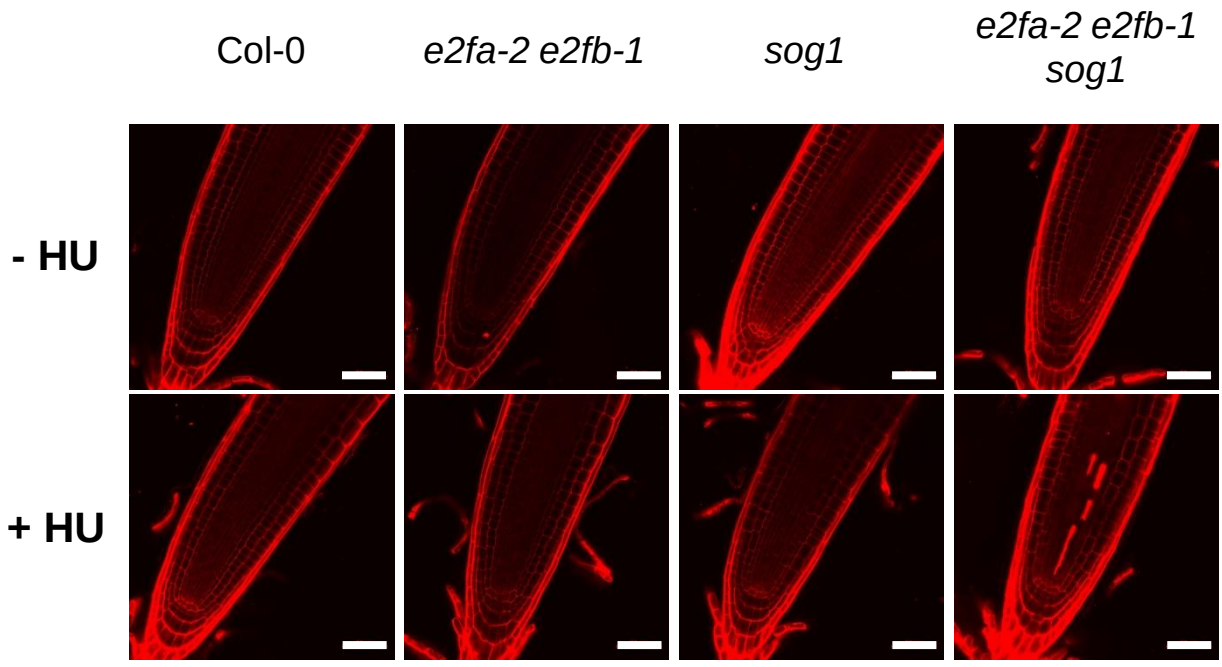


**Supplemental Figure S7: *e2fa-2 e2fb-1 sog1* triple mutants are hypersensitive to replication stress.**

Confocal images of 7-day-old *e2fa-2 e2fb-1 sog1* seedlings transferred for 24 h to control medium (- HU) or medium containing 1 mM HU (+ HU), stained with propidium iodide. Bar = 50µm for all panels.

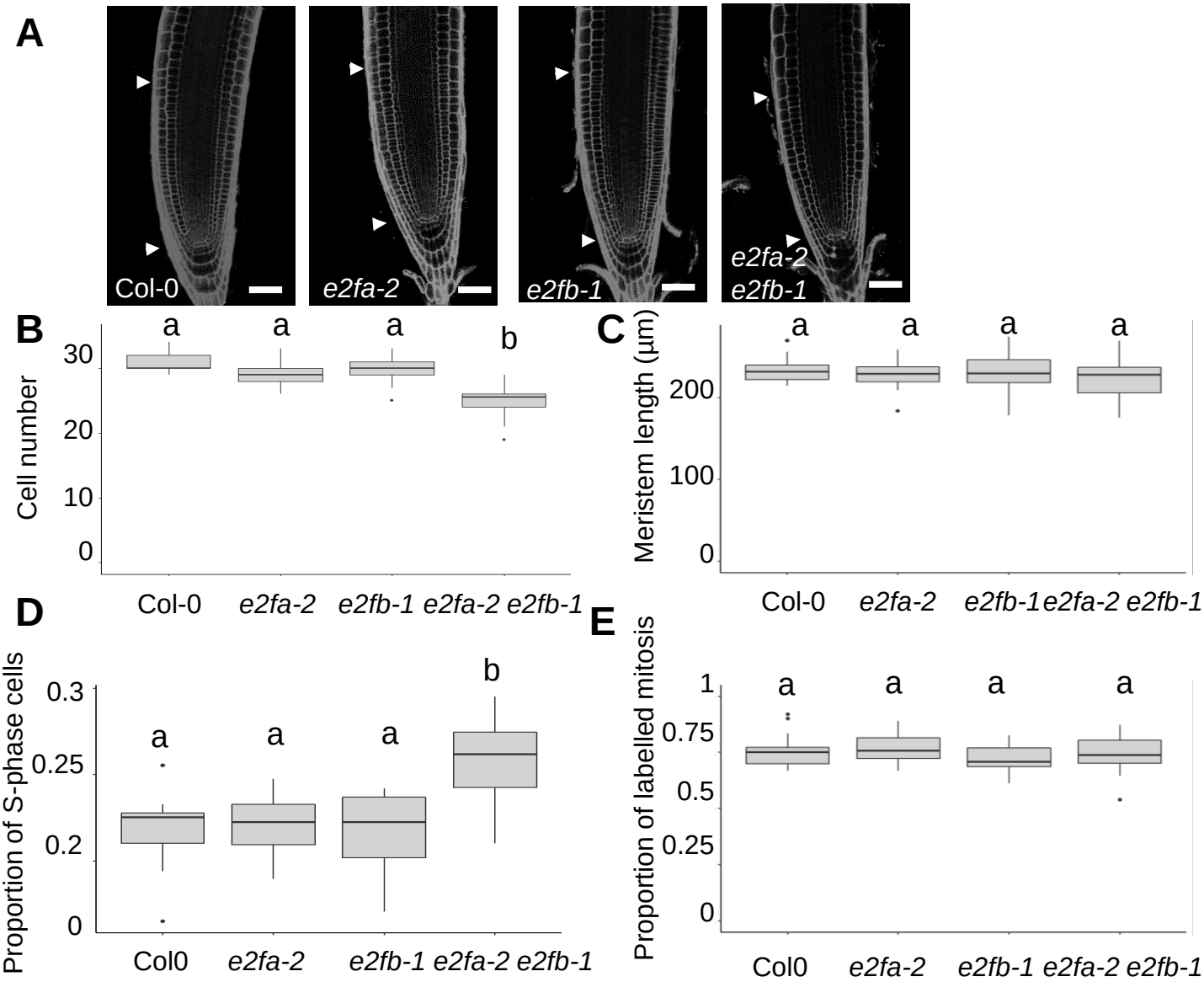


**Supplemental Figure S8. The *e2fa-2 e2fb-1* double knockout, but not single mutants, tends to have fewer cells in root meristems and longer S-phase.**

A: Confocal images of the root tips of 7-day-old wild-type (Col-0), *e2fa-2*, *e2fb-1* and *e2fa-2 e2fb-1* seedlings, Bar= 50µm for all panels.

B: Meristematic cortical cells were counted in the roots (n > 25). Different letters indicate statistically significant differences (Kruskal-Wallis test followed by Wilcoxon post-hoc test with Benjamini-Hochberg correction).

C: Meristem length was measured in the roots (n>25). No statistically significant differences were found after ANOVA analysis p>0.05.

D: The proportion of S-phase cells in increased in *e2fa2 e2fb1* root meristems, indicating that S-phase represents an increased proportion of the total cell cycle length. Plantlets were labelled with EdU for 30 min, and the proportion of positive cells was assessed in at least 10 root tips.

E: The proportion of labelled mitosis observed after 30 min EdU labelling followed by a 5h Thymidine chase does not differ between Col-0, *e2fa-2*, *e2fb-1* and *e2fa-2 e2fb-1* double mutants. In D and E, different letters indicate statistically significant differences (binomial ANOVA followed by Tukey post-hoc test p<0.01).

For all boxplots, the vertical size of the boxes shows the interquartile range, and the whiskers correspond to 1.5x the IQR. The horizontal line corresponds to the median. Individual dots indicate values falling outside of this range.